ELSEVIER

Contents lists available at ScienceDirect

## Nonlinear Analysis: Hybrid Systems

journal homepage: www.elsevier.com/locate/nahs



# Tractable model discrimination for safety-critical systems with disjunctive and coupled constraints



Qiang Shen <sup>a</sup>, Ruochen Niu <sup>b</sup>, Sze Zheng Yong <sup>b,\*</sup>

- <sup>a</sup> School of Aeronautics and Astronautics, Shanghai Jiao Tong University, 800 Dongchuan Road, Shanghai, 200240, PR China <sup>b</sup> School for Engineering of Matter, Transport and Energy, Arizona State University, 501 E Tyler Mall, Tempe, AZ, 85281, USA
- ARTICLE INFO

Article history:
Received 15 February 2021
Received in revised form 5 February 2022
Accepted 12 May 2022
Available online 6 June 2022

MSC: 00-01 99-00

Keywords: Model discrimination Input design Intention identification Fault diagnosis Autonomous driving

#### ABSTRACT

This paper considers the model discrimination problem among a finite number of models in safety-critical systems that are subjected to constraints that can be disjunctive and where state and input constraints can be coupled with each other. In particular, we consider both the optimal input design problem for active model discrimination that is solved offline as well as the online passive model discrimination problem via a model invalidation framework. To overcome the issues associated with non-convex and generalized semi-infinite constraints due to the disjunctive and coupled constraints, we propose some techniques for reformulating these constraints in a computationally tractable manner by leveraging the Karush-Kuhn-Tucker (KKT) conditions and introducing binary variables, thus recasting the active and passive model discrimination problems into tractable mixed-integer linear/quadratic programming (MILP/MIQP) problems. When compared with existing approaches, our method is able to obtain the optimal solution and is observed in simulations to also result in less computation time. Finally, we demonstrate the effectiveness of the proposed active model discrimination approach for estimating driver intention with disjunctive safety constraints and state-input coupled curvature constraints, as well as for fault identification.

© 2022 Elsevier Ltd. All rights reserved.

#### 1. Introduction

The ability to interact with the physical world through communication and control is a key enabler for future technology developments in cyber–physical systems (CPS). However, the models or behaviors of other physical systems in the shared environment may not be accessible or may only be partially observed and measured, such as intentions, faults and modes of operation. To improve CPS safety, robustness and resilience, model discrimination is used to determine the true system behavior from a set of possibilities quickly and accurately despite uncertainties, disturbances and noise.

Literature Review: Model discrimination is a widely used tool in safety–critical systems, such as CPS, robotics, chemical processes, etc., for detecting faults, attacks, and system operating modes. The methods for model discrimination can be generally categorized as either passive or active. Passive approaches, also known as model (in)validation methods, separate models by exploiting the input–output data and priori information of the system [1–7]. In [2], the definition of input-distinguishability of two linear models in a fixed time horizon was proposed and the necessary and sufficient conditions for the distinguishability were also presented. In [3], the strict residual distinguishability of continuous-time switched linear systems with deterministic disturbances was studied by defining an index for quantifying the degree

E-mail addresses: qiangshen@sjtu.edu.cn (Q. Shen), rniu6@asu.edu (R. Niu), szyong@asu.edu (S.Z. Yong).

<sup>\*</sup> Corresponding author.

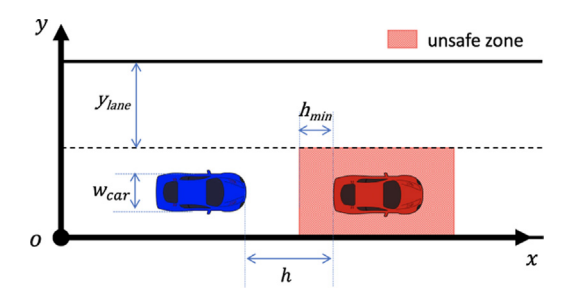


Fig. 1. Coordinate frame for an overtaking scenario. (For interpretation of the references to color in this figure legend, the reader is referred to the web version of this article.)

of residual distinguishability. In [4], a distinguishability index that measures the separation between normal models and faulty models was introduced by formulating a *T*-distinguishability optimization problem. In [5], by abstracting the nonlinear system as a piecewise linear inclusion system, the model invalidation problem identifying the true intention of nonlinear models is solved as a mixed-integer linear program (MILP). Novel frameworks of the biochemical reaction networks with sparse noisy experimental data [6] and combining qualitative information and semi-quantitative data [7] were also introduced in the area of passive model discrimination. Although passive approaches are broadly studied and often effective, they are limited to problems with specific system properties and may require a long time for discrimination since only observations are used regardless of inputs [8,9].

On the other hand, active approaches synthesize an optimal input with minimal intervention to the system dynamics such that behaviors or outputs of all models are differentiated. In the context of active fault detection, [10–12] proposed a framework for active model discrimination that obtains the small excitation that has a minimal effect on the desired behavior of the system and guarantees the isolation of different fault models. In contrast to previous approaches in [10,11], our approach does not require or compute an explicit set representation of states, while recent works that consider implicit representations of convex polyhedrons [13–16] cannot handle disjunctive and coupled constraints considered in this paper. Moreover, the stochastic approach in [12] also does not apply to the polyhedral constraints that we consider. Although we found that [17] can handle disjunctive and coupled constraints for safety–critical systems, this method is iterative and leverages a sequence of restrictions and can only obtain a suboptimal solution with the additional condition that the first restriction iteration is feasible.

Contributions: We propose optimization-based methods for active and passive model discrimination among a finite number of affine models subject to safety constraints that can be disjunctive and where constraints on states and inputs can be coupled with each other. These more general constraints in safety-critical systems can be used to represent coupled piecewise state-input constraints and disjunctive constraints. However, they often lead to generalized semi-infinite constraints (cf. [18] and references therein), which, in turn, leads to a bilevel optimization problem or a Stackelberg game. In this paper, we reformulate these constraints in a computationally tractable manner, so that the active and passive model discrimination problems can be cast into a tractable MILP problems (or MIQP when we have a quadratic objective function). The contributions of this paper are as follows:

- 1. Comparing with standard frameworks of both passive model discrimination [1,4] and active model discrimination [13,15], the proposed approaches are applicable to systems with disjunctive and coupled constraints. These more general and practical constraints can represent (coupled) state-dependent input constraints, e.g., curvature constraints or input saturation, as well as disjunctive state constraints, e.g., non-convex safety restrictions or collision-free regions.
- 2. By leveraging the KKT conditions and introducing binary variables, our proposed approach formulates a single tractable MILP/MIQP program to solve the non-convex active model discrimination problem optimally, while the existing approach in [17] is iterative and has no optimality nor feasibility guarantees.

Finally, we demonstrate the effectiveness of the proposed active and passive model discrimination approaches to discern the intentions of other human-driven or autonomous vehicles in an overtaking scenario subject to state-dependent input constraints and disjunctive (non-convex) safety constraints, as well as to detect and identify fault models of a permanent magnet DC motor.

## 2. Motivating example

While our proposed approach is applicable to a broad range of model discrimination problems, including for fault diagnosis, we begin with a motivating example of intention estimation that also serves as an example for elucidating the modeling framework with disjunctive and coupled constraints that we will introduce in Section 3.2. In particular, we consider an overtaking scenario (see Fig. 1) where the ego car (in blue) is overtaking the other car (in red). The other car's

intention (representing its driving behavior) is unknown to the ego car. The equations of motion for this two-car system are given by

$$v_{xe}(k+1) = (1 - C_d \delta t) v_{xe}(k) + u_{xe}(k) \delta t + w_{xe}(k) \delta t,$$

$$y_e(k+1) = y_e(k) + v_{ye}(k) \delta t + w_{ye}(k) \delta t,$$

$$h(k+1) = h(k) - v_{xe}(k) \delta t + v_{xo}(k) \delta t,$$

$$v_{xo}(k+1) = (1 - C_d \delta t) v_{xo}(k) + u_{xo}(k) \delta t + w_{xo}(k) \delta t,$$
(1)

where  $v_{xe}$  is ego car's longitudinal velocity,  $y_e$  is the lateral position of the ego car's geometric center, h is the headway between both cars,  $v_{xo}$  is the other car's longitudinal velocity,  $u_{xe}$  and  $v_{ye}$  are ego car's longitudinal acceleration inputs and lateral velocity inputs,  $v_{xo}$  is other car's longitudinal acceleration input,  $v_{xe}$ ,  $v_{ye}$  and  $v_{xo}$  are process noises,  $v_{xo}$  is the drag coefficient, and  $v_{xo}$  is the sampling time.

As shown in Fig. 1, to ensure safety of the two cars and avoid entering into the unsafe zone, when the ego car attempts to overtake the other car, the headway h and the ego car's lateral position  $y_e$  must satisfy the following *disjunctive* safety constraint:

$$S = \{(h, y_e) \in \mathbb{R} \times \mathbb{R} : h > h_{min} \vee y_e > \frac{1}{2} w_{car} + y_{lane}\},\tag{2}$$

where  $w_{car}$  and  $y_{lane}$  are car and lane widths. The above disjunctive safety constraint requires that the ego car stays behind the other car and maintains a safe headway (i.e.,  $h > h_{min}$ ) or drives to the side of the other car while maintaining a safe lateral distance (i.e.,  $y_e > \frac{1}{2}w_{car} + y_{lane}$ ).

In addition, to make the car model more realistic, the velocity of the ego car in the lateral direction is required to satisfy the following constraints:

$$v_{ye} \in \begin{cases} \{0\}, & v_e^{min} \le v_{xe} \le v_{xe}^{dz}, \\ \{v_{ye} : \beta_1(v_{xe} - v_{xe}^{dz}) \le v_{ye} \le \beta_2(v_{xe} - v_{xe}^{dz})\}, & v_{xe}^{dz} \le v_{xe} \le v_e^{max}, \end{cases}$$
(3)

where  $v_{xe}^{dz}$  is a dead-zone threshold (to emulate the more realistic setting where cars cannot move laterally without moving longitudinally), and  $\beta_1$  and  $\beta_2$  are slopes that mimic the curvature constraints of real cars. Since  $v_{xe}$  is the state of the ego car, this input constraint turns out to be state-dependent, i.e., there is a *coupled* state-input constraint.

Moreover, the other car may have one of the following two intentions that determine the choice of their inputs  $u_{xo}$ :

- An annoying driver who speeds up to prevent being overtaken;
- A cautious driver who slows down such that the ego car can overtake more easily.

To improve the ego car's driving safety and performance, the problems of active and passive model discrimination for inferring the intention of the other car in an overtaking scenario are considered. The objective of active model discrimination is to design a separating input offline/at design time for the ego car to identify other car's unknown intention over a fixed horizon, while satisfying disjunctive and coupled constraints. Then, the real-time input–output data generated by applying the separating input from active model discrimination is leveraged to (passively) identify the other car's true intention at run time.

#### 3. Preliminaries

In this section, we introduce some notations, definitions and useful constraint reformulations, as well as describe the modeling framework we consider.

## 3.1. Notation and definitions

Let  $x \in \mathbb{R}^n$  denote a vector and  $M \in \mathbb{R}^{n \times m}$  a matrix, with transpose  $M^T$  and  $M \ge 0$  denotes element-wise non-negativity. The set of positive integers up to n is denoted by  $\mathbb{Z}_n^+$ , and the set of non-negative integers up to n is denoted by  $\mathbb{Z}_n^0$ . The diag and vec operators are defined for a collection of matrices  $M_i$ ,  $i = 1, \ldots, n$  and matrix M as:

$$\operatorname{diag}_{k=i}^{n}\{M_{k}\} = \begin{bmatrix} M_{i} & & \\ & \ddots & \\ & & M_{n} \end{bmatrix}, \underset{k=i}{\text{vec}}\{M_{k}\} = \begin{bmatrix} M_{i} & \\ \vdots & \\ M_{n} \end{bmatrix},$$
$$\underset{k=\{i,j\}}{\operatorname{diag}}\{M_{k}\} = \begin{bmatrix} M_{i} & \mathbf{0} \\ \mathbf{0} & M_{j} \end{bmatrix}, \underset{k=\{i,j\}}{\text{vec}}\{M_{k}\} = \begin{bmatrix} M_{i} \\ M_{j} \end{bmatrix},$$
$$\underset{n}{\operatorname{diag}}\{M\} = \mathbb{I}_{n} \otimes M, \underset{n}{\text{vec}}\{M\} = \mathbb{I}_{n} \otimes M,$$

where  $\otimes$  is the Kronecker product, while  $\mathbf{0}$ ,  $\mathbb{I}_n$  and  $\mathbb{I}_n$  represent the matrix of zeros of appropriate dimensions, the vector of ones and the identity matrix of dimension n, respectively. The binomial coefficient is denoted by  $\binom{n}{k}$ , which is the number of combinations of n items taken k at a time.

We will also make use of Special Ordered Set of degree 1 (SOS-1) constraint, which is defined as follows:

**Definition 1** (SOS-1 Constraint [19]). A special ordered set of degree 1 (SOS-1) constraint is a set of integer, continuous or mixed-integer scalar variables for which at most one variable in the set may take a value other than zero, denoted as SOS-1:  $\{v_1, \ldots, v_N\}$ . For instance, if  $v_i \neq 0$ , then this constraint imposes that  $v_j = 0$  for all  $j \neq i$ , i.e.,  $v_1 = \cdots = v_{i-1} = v_{i+1} = \cdots = v_N = 0$ .

#### 3.2. Modeling framework

Consider N discrete-time affine time-invariant models  $\mathcal{G}_i = (A_i, B_i, B_{w,i}, C_i, D_i, f_i, g_i)$  over a time horizon of length T with model indicator  $i \in \mathbb{Z}_N^+$ , each with states  $\underline{\mathbf{x}}_i \in \mathbb{R}^n$ , measurements/outputs  $z_i \in \mathbb{R}^{n_z}$ , inputs  $\underline{\mathbf{u}}_i \in \mathbb{R}^m$ , process noise  $w_i \in \mathbb{R}^{m_w}$ , measurement noise  $v_i \in \mathbb{R}^{m_v}$ , constant fault or additive bias  $f_i \in \mathbb{R}^n$ ,  $g_i \in \mathbb{R}^{n_z}$ . The models evolve according to the following state and output equations:

$$\mathbf{x}_i(k+1) = A_i \mathbf{x}_i(k) + B_i \mathbf{u}_i(k) + B_{iv} i w_i(k) + f_i, \tag{4}$$

$$z_i(k) = C_i \mathbf{x}_i(k) + D_i \mathbf{u}_i(k) + D_{v,i} v_i(k) + g_i. \tag{5}$$

In the context of the motivating example, each model can represent a two-car system in (1) with  $\underline{\mathbf{x}}_i(k) \triangleq \begin{bmatrix} v_{xe}(k) & y_e(k) & h(k) & v_{xo}(k) \end{bmatrix}^{\top}$  including both states of the ego car and the other car and different  $u_{xo}$  corresponding to different other car's intentions. The states  $\underline{\mathbf{x}}_i$  can be divided into the controlled states  $x_i \in \mathbb{R}^{n_x}$  and uncontrolled states  $y_i \in \mathbb{R}^{n_y}$  with  $n_y = n - n_x$  (e.g., ego and other cars' states in the motivating example, respectively) accordingly. Similarly, the first  $m_u$  components of  $\underline{\mathbf{u}}_i$  are controlled inputs (i.e., to be designed as separating inputs), denoted as  $u \in \mathbb{R}^{m_u}$  that are the same for all  $\underline{\mathbf{u}}_i$ , while the other  $m_d = m - m_u$  components of  $\underline{\mathbf{u}}_i$ , denoted as  $d_i \in \mathbb{R}^{m_d}$ , are uncontrolled inputs that are model-dependent. For instance, u represents the ego car's inputs while  $d_i$  is the other car's inputs. As a consequence, we have

$$\underline{\boldsymbol{x}}_{i}(k) \triangleq \begin{bmatrix} x_{i}(k) \\ y_{i}(k) \end{bmatrix}, \underline{\boldsymbol{u}}_{i}(k) \triangleq \begin{bmatrix} u(k) \\ d_{i}(k) \end{bmatrix}. \tag{6}$$

Dividing the states and inputs into controlled and uncontrolled parts, the state and output equations in (4) and (5) become:

$$\underline{\boldsymbol{x}}_{i}(k+1) = \begin{bmatrix} A_{xx,i} & A_{xy,i} \\ A_{yx,i} & A_{yy,i} \end{bmatrix} \underline{\boldsymbol{x}}_{i}(k) + \begin{bmatrix} B_{xu,i} & B_{xd,i} \\ B_{yu,i} & B_{yd,i} \end{bmatrix} \underline{\boldsymbol{u}}_{i}(k) + \begin{bmatrix} B_{xw,i} \\ B_{yw,i} \end{bmatrix} w_{i}(k) + \begin{bmatrix} f_{x,i} \\ f_{y,i} \end{bmatrix}, \tag{7}$$

$$z_i(k) = C_i \underline{\mathbf{x}}_i(k) + \begin{bmatrix} D_{u,i} & D_{d,i} \end{bmatrix} \underline{\mathbf{u}}_i(k) + D_{v,i} v_i(k) + g_i.$$
(8)

The initial condition for the model i, denoted by  $\underline{\mathbf{x}}_i^0 = \underline{\mathbf{x}}_i(0)$ , is constrained to a polyhedral set with  $c_0$  inequalities:

$$\underline{\mathbf{x}}_{i}^{0} \in \mathcal{X}_{0} := \{\underline{\mathbf{x}} \in \mathbb{R}^{n} : P_{0}\underline{\mathbf{x}} \leq p_{0}\}, \ \forall i \in \mathbb{Z}_{N}^{+}. \tag{9}$$

To have a realistic model, the states  $x_i$  and  $y_i$  satisfy polyhedral state constraints with  $c_x$  and  $c_y$  inequalities:

$$x_i(k) \in \mathcal{X}_{x,i} := \{x \in \mathbb{R}^{n_x} : P_{x,i}x < p_{x,i}\},\tag{10}$$

$$y_i(k) \in \mathcal{X}_{y,i} := \{ y \in \mathbb{R}^{n_y} : P_{y,i} y \le p_{y,i} \},$$
 (11)

for  $k \in \mathbb{Z}_T^+$ . For example, (10) and (11) represent the individual constraints that the ego and other cars have to satisfy their own speed limits.

The controlled states  $x_i$  must also satisfy  $n_s$  disjunctive constraints, each with  $c_s$  inequalities:

$$x_i(k) \in \bigvee_{i=1}^{n_s} \left( \mathcal{S}_i^{(j)} := \{ x \in \mathbb{R}^{n_x} : P_{s,i}^{(j)} x \le p_{s,i}^{(j)} \} \right). \tag{12}$$

The disjunctive constraints (cf. (2) in the motivating example) are used to represent nonconvex safety restrictions or collision-free regions, where at least one constraint must be satisfied for safety, similar to logical "OR" statements.

In addition, the controlled input is subject to the following coupled state–input constraints (for  $k \in \mathbb{Z}_{T-1}^0$  and  $i \in \mathbb{Z}_N^+$ ):

$$u(k) \in \mathcal{U} := \left\{ u \in \mathbb{R}^{m_u} : \{ x_i \in \mathcal{X}_{x,i}, \forall j \in \mathbb{Z}_{n_{p,i}}^+ : Q_{ux,i}^{(j)} x_i + Q_{uu,i}^{(j)} u \le q_{u,i}^{(j)}, \text{ if } P_{ux,i}^{(j)} x_i \le p_{ux,i}^{(j)} \} \right\}, \tag{13}$$

<sup>&</sup>lt;sup>1</sup> Off-the-shelf solvers such as Gurobi and CPLEX [19,20] can readily handle these constraints, which can significantly reduce the search space for integer variables in branch and bound algorithms.

where  $x_i$  is the controlled state satisfying  $x_i \in \mathcal{X}_{x,i}$ ,  $P_{ux,i}^{(j)} x_i \leq p_{ux,i}^{(j)}$  is the jth partition of the polyhedral set  $\mathcal{X}_{x,i}$  with  $\bigcup_{j \in \mathbb{Z}_{p_1,i}^+} \{P_{ux,i}^{(j)} x_i \leq p_{ux,i}^{(j)} \}$ ,  $n_{p,i}$  is the number of partitions,  $Q_{ux,i}^{(j)} \in \mathbb{R}^{c_{p_1}^{(j)} \times n_x}$ ,  $Q_{uu,i}^{(j)} \in \mathbb{R}^{c_{p_1}^{(j)} \times m_u}$ ,  $P_{ux,i}^{(j)} \in \mathbb{R}^{c_{p_2}^{(j)} \times n_x}$ ,  $Q_{ux,i}^{(j)} \in \mathbb{R}^{c_{p_1}^{(j)} \times n_x}$ ,  $Q_{ux,i}^{(j)} \in \mathbb{R}^{c_{p_1}^{($ 

 $\mathbb{R}^{\mathfrak{c}_{p2}^{0/2}}$ . These coupled state–input constraints can incorporate more realistic constraints, e.g., curvature constraints and input saturation, with "IF-ELSE" statements. For example, considering the coupled constraint (3) in the motivating example with  $x_i = v_{xe}$  and  $u = v_{ye}$ , we have two partitions defined by  $Q_{ux,i}^{(1)} = [\beta_1; -\beta_2]$ ,  $Q_{uu,i}^{(1)} = [-1; 1]$ ,  $q_{u,i}^{(1)} = [\beta_1 v_{xe}^{dz}; -\beta_2 v_{xe}^{dz}]$ ,  $P_{ux,i}^{(1)} = [1; -1]$ ,  $P_{ux,i}^{(1)} = [v_e^{max}; -v_{xe}^{dz}]$ , and  $P_{ux,i}^{(2)} = [0; 0]$ ,  $P_{uu,i}^{(2)} = [0; 0]$ ,  $P_{ux,i}^{(2)} = [0; 0]$ , with

$$d_i(k) \in \mathcal{D}_i := \{ d \in \mathbb{R}^{m_d} : Q_{d,i} d \le q_{d,i} \}. \tag{14}$$

The process and measurement noises,  $w_i$  and  $v_i$ , are also polyhedrally constrained with  $c_w$  and  $c_v$  inequalities:

$$w_i(k) \in \mathcal{W}_i := \{ w \in \mathbb{R}^{m_w} : Q_{w,i} w \le q_{w,i} \}, \tag{15}$$

$$v_i(k) \in \mathcal{V}_i := \{ v \in \mathbb{R}^{m_v} : Q_{v,i} v \le q_{v,i} \}.$$
 (16)

#### 3.3. Concatenated models and constraints

Next, we will introduce some time-concatenated and pair-concatenated notions. The time-concatenated states and outputs over the time horizon T are defined as

$$\underline{\mathbf{x}}_{i,T} = \underset{k=0}{\text{vec}} \{\underline{\mathbf{x}}_i(k)\}, \quad x_{i,T} = \underset{k=0}{\text{vec}} \{x_i(k)\},$$
$$y_{i,T} = \underset{k=0}{\text{vec}} \{y_i(k)\}, \quad z_{i,T} = \underset{k=0}{\text{vec}} \{z_i(k)\},$$

while the time-concatenated inputs and noises are defined as

$$\underline{\mathbf{u}}_{i,T} = \bigvee_{\substack{k=0 \\ k=0}}^{T-1} \{\underline{\mathbf{u}}_{i}(k)\}, u_{T} = \bigvee_{\substack{k=0 \\ k=0}}^{T-1} \{u(k)\}, 
d_{i,T} = \bigvee_{\substack{k=0 \\ k=0}}^{T-1} \{d_{i}(k)\}, w_{i,T} = \bigvee_{\substack{k=0 \\ k=0}}^{T-1} \{w_{i}(k)\}, 
v_{i,T} = \bigvee_{\substack{k=0 \\ k=0}}^{T} \{v_{i}(k)\}.$$

To separate all models, we further introduce the model pair, which consists of two different models of  $\mathcal{G}_i$ ,  $\forall i \in \mathbb{Z}_N^+$ . Considering N discrete-time affine models, i.e.,  $\mathcal{G}_1$ ,  $\mathcal{G}_2$ ,  $\cdots$ ,  $\mathcal{G}_N$ , there are  $I = \binom{N}{2}$  model pairs and let the mode  $\iota \in \{1, \ldots, I\}$ denote the pair of models  $(G_i, G_j)$ . Then, concatenating  $\mathbf{x}_i^0, \mathbf{x}_{i,T}, x_{i,T}, y_{i,T}, d_{i,T}, z_{i,T}, w_{i,T}$  and  $v_{i,T}$  for each model pair, we define

$$\underline{\mathbf{x}}_{0}^{t} = \underset{k=\{i,j\}}{\text{vec}} \{\underline{\mathbf{x}}_{k}^{0}\}, \underline{\mathbf{x}}_{T}^{t} = \underset{k=\{i,j\}}{\text{vec}} \{\underline{\mathbf{x}}_{k,T}\}, x_{T}^{t} = \underset{k=\{i,j\}}{\text{vec}} \{x_{k,T}\}, 
y_{T}^{t} = \underset{k=\{i,j\}}{\text{vec}} \{y_{k,T}\}, z_{T}^{t} = \underset{k=\{i,j\}}{\text{vec}} \{z_{k,T}\}, d_{T}^{t} = \underset{k=\{i,j\}}{\text{vec}} \{d_{k,T}\}, 
w_{T}^{t} = \underset{k=\{i,j\}}{\text{vec}} \{w_{k,T}\}, v_{T}^{t} = \underset{k=\{i,j\}}{\text{vec}} \{v_{k,T}\}.$$

Thus, the pair-concatenated dynamics, in which states and outputs over the entire time horizon for each model pair  $\iota$ are written as simple functions of the initial state  $\underline{x}_0^\iota$ , input vectors  $u_T$ ,  $d_T^\iota$ , and noise  $w_T^\iota$ ,  $v_T^\iota$ , is given by:

$$\mathbf{x}_{T}^{t} = M_{\mathbf{x}}^{t} \mathbf{\underline{x}}_{0}^{t} + \Gamma_{\mathbf{x}u}^{t} \mathbf{u}_{T} + \Gamma_{\mathbf{x}d}^{t} \mathbf{d}_{T}^{t} + \Gamma_{\mathbf{x}w}^{t} \mathbf{w}_{T}^{t} + \tilde{\mathbf{f}}_{\mathbf{x}}^{t}, \tag{17}$$

$$y_{t}^{t} = M_{v}^{t} \mathbf{x}_{0}^{t} + \Gamma_{vu}^{t} u_{T} + \Gamma_{vd}^{t} d_{T}^{t} + \Gamma_{vu}^{t} w_{T}^{t} + \tilde{f}_{v}^{t}, \tag{18}$$

$$\mathbf{x}_{t}^{t} = \bar{A}^{t}\mathbf{x}_{0}^{t} + \Gamma_{t}^{t}u_{T} + \Gamma_{t}^{t}d_{T}^{t} + \Gamma_{c}^{t}w_{T}^{t} + \tilde{f}^{t}, \tag{19}$$

$$z_t^t = \bar{C}^t \mathbf{x}_t^t + \bar{D}_u^t u_T + \bar{D}_d^t d_T + \bar{D}_u^t v_T^t + \tilde{g}^t, \tag{20}$$

where the involved matrices and vectors, as well as the procedures for deriving them are given in Appendix A.

In addition, the uncertain variables for each model pair  $\iota$  are concatenated as  $\vec{x}^{\iota} = [\underline{x}_{0}^{\iota T} \ d_{T}^{\iota T} \ w_{T}^{\iota T} \ v_{T}^{\iota T}]^{\mathsf{T}}$ . Therefore, the pair-concatenated constraints on states  $\dagger \in \{x, y\}$  and uncertainties can be rewritten as

$$H_{\uparrow}^{\iota} \vec{X}^{\iota} \leq \bar{p}_{\uparrow}^{\iota} - \bar{P}_{\uparrow}^{\iota} \tilde{f}_{\uparrow}^{\iota} - \bar{P}_{\uparrow}^{\iota} \Gamma_{\uparrow u}^{\iota} u_{T}, \quad H_{\overline{X}}^{\iota} \vec{X}^{\iota} \leq h_{\overline{X}}^{\iota}, \tag{21}$$

where the definitions for the matrices and vectors  $H_{\dagger}^{\iota}$ ,  $\bar{P}_{\dagger}^{\iota}$ ,  $\Gamma_{\dagger u}^{\iota}$ ,  $\bar{p}_{\dagger}^{\iota}$ ,  $H_{\overline{x}}^{\iota}$  and  $h_{\overline{x}}^{\iota}$ , as well as the procedures for their derivation can be found in Appendix B.

Furthermore, to reformulate coupled state-input constraints, we define  $\bar{\bar{x}}_{i,k} = \begin{bmatrix} \underline{\mathbf{x}}_i^{0\mathsf{T}} & d_{i,0:k-1}^{\mathsf{T}} & w_{i,0:k-1}^{\mathsf{T}} \end{bmatrix}^{\mathsf{T}}$  satisfying  $H_{\bar{z}_{i,k}}, \bar{\bar{x}}_{i,k} \leq h_{\bar{z}_{i,k}}$ , where

$$H_{\bar{z}_{ik}} = \text{diag}\{P_0, \bar{Q}_{d,i,k}, \bar{Q}_{w,i,k}\}, \tag{22}$$

$$h_{\bar{x},i,k} = \text{vec}\{p_0, \bar{q}_{d,i,k}, \bar{q}_{w,i,k}\},$$
 (23)

with  $\bar{Q}_{d,i,k} = \operatorname{diag}_{k+1}\{Q_{d,i}\}, \ \bar{Q}_{w,i,k} = \operatorname{diag}_{k+1}\{Q_{w,i}\}, \ \bar{q}_{d,i,k} = \operatorname{vec}_{k+1}\{q_{d,i}\}, \ \bar{q}_{w,i,k} = \operatorname{vec}_{k+1}\{q_{w,i}\}, \ d_{i,0:k-1} = \operatorname{vec}_{t=0}^{k-1}\{d_i(t)\}, \ w_{i,0:k-1} = \operatorname{vec}_{t=0}^{k-1}\{w_i(t)\}, \ d_{0:-1} = 0, \ \text{and} \ w_{0:-1} = 0.$  Then, we rewrite the controlled and uncontrolled states, x and y, at time instant  $k \in \mathbb{Z}_{T-1}^0$  for model  $\mathcal{G}_i$  as

$$\dagger_{i}(k) = M_{\bar{\dagger}_{i,k}} \bar{\bar{x}}_{i,k} + \Gamma_{\dagger u,i,k} u_{0:k-1} + \tilde{f}_{\dagger,i,k}, \tag{24}$$

where  $\dagger \in \{x, y\}$ ,  $M_{\overline{f}_{i,k}} = \begin{bmatrix} M_{\dagger,i,k} & \Gamma_{\dagger d,i,k} & \Gamma_{\dagger w,i,k} \end{bmatrix}$ ,  $u_{0:k-1} = \text{vec}_{t=0}^{k-1}\{u(t)\}$ , and  $u_{0:-1} = 0$ . Defining  $\Upsilon_{\dagger k} = b_k \otimes I_{n_{\dagger}}$  with  $b_k \in \mathbb{R}^T$  being the ith basis row vector in  $\mathbb{R}^T$ , we have  $M_{\dagger,i,k} = \Upsilon_{\dagger k} M_{\dagger,i,T}$ ,  $\Gamma_{\dagger \star,i,k} = \Upsilon_{\dagger k} \Gamma_{\dagger \star,i,T}$ ,  $\tilde{f}_{\dagger,i,k} = \Upsilon_{\dagger k} \tilde{f}_{\dagger,i,T}$ .

 $b_k \in \mathbb{R}^T$  being the ith basis row vector in  $\mathbb{R}^T$ , we have  $M_{\uparrow,i,k} = \Upsilon_{\uparrow k} M_{\uparrow,i,T}$ ,  $\Gamma_{\uparrow\star,i,k} = \Upsilon_{\uparrow k} \Gamma_{\uparrow\star,i,T}$ ,  $\tilde{f}_{\uparrow,i,k} = \Upsilon_{\uparrow k} \tilde{f}_{\uparrow,i,T}$ . Then, the coupled input–state piecewise constraints in (13) for each time instant  $k \in \mathbb{Z}^0_{T-1}$  and model  $i \in \mathbb{Z}^+_N$  with respect to  $\overline{\bar{x}}_{i,k}$  and  $u_T$  are given by

$$\left\{ \forall j \in \mathbb{Z}_{n_{p,i}}^{+} : Q_{ux,i}^{(j)} M_{\overline{\tilde{\chi}}_{i,k}} \overline{\tilde{\tilde{\chi}}}_{i,k} + \begin{bmatrix} Q_{ux,i}^{(j)} \Gamma_{xu,i,k} & Q_{uu,i}^{(j)} & 0 \end{bmatrix} u_{T} \leq q_{u,i}^{(j)} - Q_{ux,i}^{(j)} \tilde{\tilde{f}}_{x,i,k}, \\
\text{if } P_{ux,i}^{(j)} M_{\overline{\tilde{\chi}}_{i,k}} \overline{\tilde{\tilde{\chi}}}_{i,k} + \begin{bmatrix} P_{ux,i}^{(j)} \Gamma_{xu,i,k} & 0 \end{bmatrix} u_{T} \leq p_{ux,i}^{(j)} - P_{ux,i}^{(j)} \tilde{\tilde{f}}_{x,i,k} \right\}.$$
(25)

Furthermore, the state constraints in (12) for each time instant  $k \in \mathbb{Z}_{T-1}^0$  and model  $i \in \mathbb{Z}_N^+$  with respect to  $\overline{\bar{x}}_{i,k}$  and  $u_T$  are rewritten as

$$\bigvee_{i=1}^{n_s} \left( P_{s,i}^{(j)} M_{\overline{x}_{i,k}} \overline{\overline{x}}_{i,k} \le p_{s,i}^{(j)} - P_{s,i}^{(j)} \widetilde{f}_{x,i,k} - P_{s,i}^{(j)} \Gamma_{xu,i,k} u_T \right). \tag{26}$$

**Remark 1.** It is important to ensure that the models are meaningful in the sense that for the range of time horizon T and for each model  $i \in \mathbb{Z}_N^+$ , (11) holds for any given  $\underline{\mathbf{x}}_0 \in \mathcal{X}_0$  that satisfies  $y_i(0) \in \mathcal{X}_{y,i}$  for all  $i \in \mathbb{Z}_N^+$ , and for any given  $u(k) \in \mathcal{U}$  for all  $k \in \mathbb{Z}_{T-1}^0$ . If the considered affine model satisfies these assumptions, we refer to it as well-posed [13]. We shall assume throughout the paper that the given affine models are always well-posed.

#### 3.4. Problem formulation

Using the framework above, we can state our active model discrimination problem as follows:

**Problem 1** (*Active Model Discrimination*). Given N well-posed affine models  $\mathcal{G}_i$  and a model separating threshold  $\epsilon$  the active model discrimination problem can be stated as follows:

$$\min_{u_{T}, x_{T}, z_{T}} J(u_{T})$$
s.t. 
$$\forall \underline{\mathbf{x}}_{i}^{0}, d_{i,T}, w_{i,T} :$$

$$(4), (6)-(7), (9), (11), (14), (15) \text{ hold}$$

$$\forall i, j \in \mathbb{Z}_{N}^{+}, i < j, \forall k \in \mathbb{Z}_{T-1}^{0},$$

$$\forall \underline{\mathbf{x}}_{i}^{0}, d_{i,T}, w_{i,T}, v_{i,T} :$$

$$(4)-(9), (11), (14)-(16) \text{ hold}$$

$$(27a)$$

$$(3k' \in \mathbb{Z}_{T}^{0} :$$

$$(27b)$$

In the above, the constraint (27a) means that for all possible realizations of initial states, uncontrolled states, uncontrolled inputs, and process noise (on the left side of the brace), the controlled state constraint (10), safety constraint (12) and state-dependent input constraint (13) should hold over the entire horizon for each intention. Meanwhile, constraint (27b) defines the model separability condition, which means that for all possible realizations of initial states, uncontrolled states, uncontrolled inputs, process noise and measurement noise, the output trajectories of all pairs of models have to differ by a threshold  $\epsilon$  in at least one time instant.

Moreover, the active model discrimination problem is intended to be solved offline to find the optimal discriminating/separating input for guaranteeing that the models are distinct, which is then used online in conjunction with a passive model discrimination algorithm for determining the true model at run time based on the observed input-output trajectory. Thus, a second problem of interest is as follows:

**Problem 2** (*Passive Model Discrimination*). Given a sequence of run-time input-output trajectory  $\{u(k), z_m(k)\}_{k=0}^{T-1}$  (u(k) is obtained from solving Problem 1 and  $z_m(k)$  is observed at run time) and N well-posed affine models  $\mathcal{G}_i$ , determine which model is consistent with the given trajectory for all possible initial states  $\mathbf{x}_i^0$ , uncontrolled inputs  $d_{i,T}$ , process noise  $w_{i,T}$ and measurement noise  $v_{i,T}$ , where a model  $\mathcal{G}_{i}$  is consistent or valid if the following is feasible:

Find 
$$\underline{\mathbf{x}}_{i}^{0}$$
,  $d_{i,T}$ ,  $w_{i,T}$ ,  $v_{i,T}$ , s.t. (7)–(16) hold. (28)

## 4. Main approach

To solve Problems 1 and 2, we propose to reformulate constraints (27a), (27b) and (28) in a computationally tractable manner. We begin by proving a few useful lemmas and propositions, and then we provide solutions to Problems 1 and 2 via Theorems 1 and 2, respectively.

## 4.1. Useful lemmas and propositions

For increased readability, the proofs for all the following lemmas and propositions are provided in the Appendices.

**Lemma 1** (Generalized Semi-infinite Constraint Reformulation). The following generalized semi-infinite constraint

$$\mathcal{A}_{\mathcal{X}} < b + C_{\mathcal{Y}}, \forall \chi \in \mathcal{X}(\mathcal{Y}) \triangleq \{ \chi : \mathcal{D}_{\mathcal{X}} < e + \mathcal{F}_{\mathcal{Y}}, G_{\mathcal{X}} < h \}$$
(29)

with variables  $\chi$  and u, matrices A, C, D, F and G, and vectors b, e and h with appropriate dimensions, can be recast as

(i) Bilinear Equivalence

$$\Pi^{\mathsf{T}} \begin{bmatrix} e + \mathcal{F}y \\ h \end{bmatrix} \le b + \mathcal{C}y, \, \Pi^{\mathsf{T}} \begin{bmatrix} \mathcal{D} \\ \mathcal{G} \end{bmatrix} = \mathcal{A}, \, \Pi \ge 0, \tag{30}$$

where  $\Pi$  is a dual matrix variable, and

(ii) Mixed-Integer Equivalence

$$p_a \le 0, \ v_{1,a} \ge 0, \ v_{2,a} \ge 0,$$
 (31a)

$$p_{a} \leq 0, \ \nu_{1,a} \geq 0, \ \nu_{2,a} \geq 0,$$

$$\forall b : 0 = \sum_{i} \nu_{1,a,i} \mathcal{D}(i,b) + \sum_{j} \nu_{2,a,j} \mathcal{G}(j,b) - \mathcal{A}(a,b),$$
(31a)

$$p_{a} = \mathcal{A}_{(a)}\chi_{a} - b_{(a)} - C_{(a)}y,$$

$$\mathcal{D}\chi_{a} \leq e + \mathcal{F}y, \ G\chi_{a} \leq h,$$
(31c)

$$\forall i: SOS-1: \{\nu_{1,a,i}, \mathcal{D}_{(i)}\chi_a - e_{(i)} - \mathcal{F}_{(i)}y\}, 
\forall j: SOS-1: \{\nu_{2,a,j}, \mathcal{G}_{(j)}\chi_a - h_{(j)}\},$$
(31d)

for all  $a \in \mathbb{Z}_{n_a}^+$ , where  $n_a$  is the number of rows of  $\mathcal{A}$ ,  $\chi_a$ ,  $\mathcal{V}_{1,a}$  and  $\mathcal{V}_{2,a}$  are additional slack variables for each a. We denote as  $\mathcal{A}_{(a)}$ ,  $\mathcal{b}_{(a)}$  and  $\mathcal{C}_{(a)}$  the a-th rows of  $\mathcal{A}$ ,  $\mathcal{b}$  and  $\mathcal{C}$ , respectively, while  $\mathcal{D}(i,b)$ ,  $\mathcal{G}(j,b)$  and  $\mathcal{A}(a,b)$  are the corresponding elements of matrices  $\mathcal{D}$ ,  $\mathcal{G}$  and  $\mathcal{A}$ , respectively.

**Remark 2.** In Equivalence (i), if  $\mathcal{F} = 0$  (corresponding to standard semi-infinite constraints; cf. [18]), the constraints are linear. However, when  $\mathcal{F} \neq 0$  (corresponding to generalized semi-infinite constraints; cf. [18]), the constraints become bilinear. To deal with these bilinear constraints, [17] proposed a sequence of restriction approach, but it can only find a feasible suboptimal solution under the condition that the first restriction does not lead to infeasibility. By contrast, our Equivalence (ii) that leverages slack variables and KKT conditions is exact for any  ${\cal F}$  and avoids the bilinear constraint in Equivalence (i), albeit with the introduction of SOS-1 constraints, which are integral constraints, leading to mixed-integer linear constraints.

**Lemma 2** (Disjunctive ("OR") Constraint Reformulation). The disjunctive constraint,  $\bigvee_i (q^{(i)} \leq 0)$ , is equivalent to

$$\forall i: \ r^{(i)} \in \{0, 1\}, \ q^{(i)} \le s^{(i)}, SOS-1: \{r^{(i)}, s^{(i)}\}, \tag{32a}$$

$$\sum_{i} r^{(i)} \ge 1. \tag{32b}$$

**Lemma 3** (Piecewise Constraint Reformulation). Given a partition  $\{S^{(i)}\chi + T^{(i)}y \leq \beta^{(i)}\}$ , the following piecewise constraint:

$$\forall i: Q^{(i)} x + \mathcal{R}^{(i)} y < \alpha^{(i)}, \text{ if } S^{(i)} x + \mathcal{T}^{(i)} y < \beta^{(i)},$$

is equivalent to

$$\forall i: \begin{cases} \gamma^{(i)} \in \{0, 1\}, SOS-1: \{\gamma^{(i)}, t^{(i)}\}, \\ \left[ \begin{matrix} \mathcal{Q}^{(i)} & \mathcal{R}^{(i)} \\ \mathcal{S}^{(i)} & \mathcal{T}^{(i)} \end{matrix} \right] \left[ \begin{matrix} \chi \\ y \end{matrix} \right] \leq \left[ \begin{matrix} \alpha^{(i)} \\ \beta^{(i)} \end{matrix} \right] + t^{(i)} \mathbb{1}, \end{cases}$$

$$(33a)$$

$$\sum_{i} \gamma^{(i)} = 1. \tag{33b}$$

Next, by leveraging the lemmas above, we provide the following propositions for reformulating the controlled states constraints (10), disjunctive safety constraints (12), coupled state–input piecewise constraints (13) in (27a) and model separability condition in (27b) of Problem 1. Note that in each of the following propositions, we assume that the other constraints in Problem 1 are satisfied. Since we enforce all constraints simultaneously, they trivially hold in the uncertainty sets of each other's propositions and need not be explicitly included.

**Proposition 1** (Polytopic State Constraint Reformulation). The polytopic state constraint, i.e., the controlled state constraint (10), in (27a) of Problem 1 is equivalent to

$$\forall i \in \mathbb{Z}_{N}^{+}, \forall a \in \mathbb{Z}_{c_{x}}^{+} :$$

$$\begin{cases} \pi_{r,a}^{i} \leq 0, v_{1,r,a}^{i} \geq 0, v_{2,r,a}^{i} \geq 0, \\ \forall b : 0 = \sum_{c} v_{1,r,a,c}^{i} H_{y}^{i}(c,b) + \sum_{d} v_{2,r,a,d}^{i} H_{\bar{x}}^{i}(d,b) - H_{x}^{i}(a,b), \\ \pi_{r,a}^{i} = (H_{x}^{i})_{(a)} \bar{x}_{a}^{i} - (\bar{p}_{x}^{i})_{(a)} + (\bar{P}_{x}^{i})_{(a)} \Gamma_{xu}^{i} u_{T}, \\ H_{y}^{i} \bar{x}_{a}^{i} \leq \bar{p}_{y}^{i} - \bar{P}_{y}^{i} \bar{f}_{y}^{i} - \bar{P}_{y}^{i} \Gamma_{yu}^{i} u_{T}, H_{\bar{x}}^{i} \bar{x}_{a}^{i} \leq h_{\bar{x}}^{i}, \\ \forall c : SOS-1 : \left\{ v_{1,r,a,c}^{i}, (H_{y}^{i})_{(c)} \bar{x}_{a}^{i} - (\bar{p}_{y}^{i})_{(c)} + (\bar{P}_{y}^{i})_{(c)} \tilde{f}_{y}^{i} + (\bar{P}_{y}^{i})_{(c)} \Gamma_{yu} u_{T} \right\},$$

$$\forall d : SOS-1 : \left\{ v_{2,r,a,d}^{i}, (H_{\bar{x}}^{i})_{(d)} \bar{x}_{a}^{i} - (h_{\bar{x}}^{i})_{(d)} \right\},$$

where the subscript r refers to polytopic state constraints.

**Proposition 2** (Disjunctive State Constraints Reformulation). The disjunctive state constraints, i.e., (12), in (27a) of Problem 1 can be reformulated as

$$\forall i \in \mathbb{Z}_{N}^{+}, \forall j \in \mathbb{Z}_{n_{s,i}}^{+}, \forall k \in \mathbb{Z}_{T-1}^{0}, \forall a \in \mathbb{Z}_{c_{s}}^{+}:$$

$$\begin{cases} r_{i,k}^{(j)} \in \{0, 1\}, SOS-1: \{r_{i,k}^{(j)}, s_{i,k}^{(j)}\}, \sum_{j} r_{i,k}^{(j)} \geq 1, \\ \pi_{s,i,a}^{(j)} \leq 0, v_{1,s,i,a}^{(j)} \geq 0, v_{2,s,i,a}^{(j)} \geq 0, \\ \forall b: 0 = \sum_{c} v_{1,s,i,a,c}^{(j)} (P_{y,i}^{(j)} M_{\overline{y}_{i,k}})(c,b) + \sum_{d} v_{2,s,i,a,d}^{(j)} (H_{\overline{x},i,k})(d,b) - (P_{s,i}^{(j)} M_{\overline{x}_{i,k}})(a,b), \\ \pi_{s,i,a}^{(j)} = (P_{s,i}^{(j)})_{(a)} M_{\overline{x}_{i,k}^{(j)}} \overline{x}_{s,i,k,a}^{(j)} + (P_{s,i}^{(j)})_{(a)} \Gamma_{xu,i,k} u_{T} - (p_{s,i}^{(j)})_{(a)} + (P_{s,i}^{(j)})_{(a)} \widetilde{f}_{x,i,k} - s_{i,k}^{(j)}, \\ P_{y,i}^{(j)} M_{\overline{y}_{i,k}} \overline{x}_{s,i,k,a}^{(j)} + P_{y,i}^{(j)} \Gamma_{yu,i,k} u_{T} - p_{y,i}^{(j)} + P_{y,j}^{(j)} \widetilde{f}_{y,i,k} \leq 0, \\ H_{\overline{x},i,k} \overline{x}_{s,i,k,a}^{(j)} - h_{\overline{x},i,k} \leq 0, \\ \forall c: SOS-1: \left\{ v_{1,s,i,a,c}^{(j)}, (P_{y,i}^{(j)})_{(c)} M_{\overline{y}_{i,k}} \overline{x}_{s,i,k,a}^{(j)} + (P_{y,i}^{(j)})_{(c)} \Gamma_{yu,i,k} u_{T} - (p_{y,i}^{(j)})_{(c)} + (P_{y,i}^{(j)})_{(c)} \widetilde{f}_{y,i,k} \right\}, \\ \forall d: SOS-1: \left\{ v_{2,s,i,a,d}^{(j)}, (H_{\overline{x},i,k})_{(d)} \overline{x}_{s,i,k,a}^{(j)} - (h_{\overline{x},i,k})_{(d)} \right\}, \end{cases}$$

where the subscript s refers to disjunctive state constraints.

**Proposition 3** (Coupled State-input Constraints Reformulation). prop:piecewise he coupled state-input constraints, i.e., (13), in (27a) of Problem 1 is equivalent to

$$\forall i \in \mathbb{Z}_{N}^{+}, \forall j \in \mathbb{Z}_{n_{p,i}}^{+}, \forall k \in \mathbb{Z}_{T-1}^{0}, \forall a \in \mathbb{Z}_{c_{p_{1}}+c_{p_{2}}}^{0} :$$

$$\begin{cases} y_{i,k}^{(j)} \in \{0,1\}, SOS-1: \{y_{i,k}^{(j)}, t_{i,k}^{(j)}, \sum_{j} y_{i,k}^{(j)} = 1, \\ \pi_{t,i,a}^{(j)} \leq 0, v_{1,t,i,a,c}^{(j)}(P_{y,i}^{(j)}M_{\overline{y}_{i,k}})(c,b) + \sum_{d} v_{2,t,i,a,d}^{(j)}(H_{\overline{x},i,k}^{-})(d,b) - \left(\begin{bmatrix} Q_{ux,i}^{(j)}M_{\overline{x}_{i,k}}^{-} \\ P_{ux,i}^{(j)}M_{\overline{x}_{i,k}}^{-} \end{bmatrix}\right)(a,b), \\ \begin{cases} \pi_{t,i,a}^{(j)} = \left(\begin{bmatrix} Q_{ux,i}^{(j)}M_{\overline{x}_{i,k}}^{-} \\ P_{y,i}^{(j)}M_{\overline{y}_{i,k}}^{-} \end{bmatrix}\right)_{(a)} \overline{\chi}_{t,i,k,a}^{(j)} - \left(\begin{bmatrix} q_{u,i}^{(j)} - Q_{ux,i}^{(j)}\tilde{f}_{x,i,k} \\ P_{ux,i}^{(j)} - P_{ux,i}^{(j)}\tilde{f}_{x,i,k} \end{bmatrix}\right)_{(a)} + \left(\begin{bmatrix} Q_{ux,i}^{(j)}T_{xu,i,k} & Q_{uu,i}^{(j)} & 0 \\ P_{ux,i}^{(j)}T_{xu,i,k} & 0 \end{bmatrix}\right) \right]_{(a)} u_{T} - t_{i,k}^{(j)}, \\ \end{cases} \\ \begin{cases} P_{y,i}^{(j)}M_{\overline{y}_{i,k}}\overline{\chi}_{t,i,k,a}^{(j)} + P_{y,i}^{(j)}T_{yu,i,k}u_{T} - p_{y,i}^{(j)} + P_{y,i}^{(j)}\tilde{f}_{y,i,k} \leq 0, \\ P_{\overline{x},i,k}\overline{\chi}_{t,i,k,a}^{(j)} - h_{\overline{x},i,k}^{-} \leq 0, \\ \forall c: SOS-1: \left\{ v_{1,t,i,a,c}^{(j)}, (P_{y,i}^{(j)})_{c}M_{\overline{y}_{i,k}}\overline{\chi}_{t,i,k,a}^{(j)} + (P_{y,i}^{(j)})_{c}T_{yu,i,k}u_{T} - (p_{y,i}^{(j)})_{c} + (P_{y,i}^{(j)})_{c}\tilde{f}_{y,i,k} \right\}, \\ \forall d: SOS-1: \left\{ v_{2,t,i,a,d}^{(j)}, (H_{\overline{x},i,k}^{-})_{d}\overline{\chi}_{t,i,k,a}^{(j)} - (h_{\overline{x},i,k}^{-})_{d} \right\}, \end{aligned}$$

where the subscript t refers to coupled input-state constraints.

**Proposition 4** (Separability Condition [13]). The separability constraint in (27b) of Problem 1 is equivalent to

$$\forall \iota \in \mathbb{Z}_I^+$$
:

$$\begin{cases} \delta^{\iota}(u_{T}) \geq \epsilon, 0 = 1 - \mu_{3}^{-1} \mathbb{1}, \\ \forall m \in \mathbb{Z}_{\eta}^{+} : 0 = \sum_{i=1}^{\kappa} \mu_{1,i}^{\iota} H_{\bar{\chi}}^{\iota}(i,m) + \sum_{j=1}^{\xi} \mu_{2,j}^{\iota} R^{\iota}(j,m) + \sum_{k=1}^{\rho} \mu_{3,k}^{\iota} R^{\iota}(\xi + k, m), \\ \forall i \in \mathbb{Z}_{\kappa}^{+} : (H_{\bar{\chi}}^{\iota})_{(i)} \bar{x}^{\iota} - (h_{\bar{\chi}}^{\iota})_{(i)} \leq 0, \mu_{1,i}^{\iota} \geq 0, \\ \forall j \in \mathbb{Z}_{\xi}^{+} : (R^{\iota})_{(j)} \bar{x}^{\iota} - (r^{\iota})_{(j)} + (S^{\iota})_{(j)} u_{T} \leq 0, \mu_{2,j}^{\iota} \geq 0, \\ \forall k \in \mathbb{Z}_{\rho}^{+} : (R^{\iota})_{(\xi + k)} \bar{x}^{\iota} - \delta^{\iota} - (r^{\iota})_{(\xi + k)} + (S^{\iota})_{(\xi + k)} u_{T} \leq 0, \mu_{3,k}^{\iota} \geq 0, \\ \forall i \in \mathbb{Z}_{\kappa}^{+} : SOS-1 : \{\mu_{1,i}^{\iota}, (H_{\bar{\chi}}^{\iota})_{(i)} \bar{x}^{\iota} - (h_{\bar{\chi}}^{\iota})_{(i)}\}, \\ \forall j \in \mathbb{Z}_{\xi}^{+} : SOS-1 : \{\mu_{2,j}^{\iota}, (R^{\iota})_{(j)} \bar{x}^{\iota} - (r^{\iota})_{(j)} + (S^{\iota})_{(j)} u_{T}\}, \\ \forall k \in \mathbb{Z}_{\rho}^{+} : SOS-1 : \{\mu_{3,k}^{\iota}, (R^{\iota})_{(\xi + k)} \bar{x}^{\iota} - \delta^{\iota} - (r^{\iota})_{(\xi + k)} + (S^{\iota})_{(\xi + k)} u_{T}\}. \end{cases}$$

where the matrix definitions can be found in Appendix C.

#### 4.2. Active model discrimination

Using Propositions 1-4, it is straightforward to show that the active model discrimination problem in Problem 1 can be recast into a tractable MILP/MIQP as follows:

**Theorem 1** (Discriminating/Separating Input Design). Given a separability index  $\epsilon$ , polytopic state constraints (10), disjunctive state constraints (12), coupled input-state constraints (13), Problem 1 is equivalent to

$$u_{T}^{*} = \arg \min_{\substack{u_{T}, \delta^{i}, \bar{x}^{i}, \mu_{\psi}^{i}, \nu_{\psi}^{(j)}, \nu_{\psi}^{(j)}, \bar{x}^{i}_{a}, \\ \bar{x}_{\phi, i, k, a}^{(j)}, s_{i, k}^{(j)}, t_{i, k}^{(j)} \in [0, 1], y_{i, k}^{(j)} \in [0, 1]}} J(u_{T})$$

$$(38a)$$

for each • ∈  $\{1, 2, 3\}$ , ∘ ∈  $\{1, 2\}$ , and ⋄ ∈  $\{r, s, t\}$ .

When compared with existing active model discrimination approaches [13,15], our approach can relax the rather limiting assumption in these works (i.e., Assumption 1 in [13,15]) that the separating input does not affect the uncontrolled state constraints, and hence, the proposed approach is applicable to more general systems.

The discriminating/separating input from the optimization problem in the above theorem that is solved offline will be applied to the system of interest and the observed measurements/outputs are obtained at run time. The collected inputoutput data will then be used at run time to determine the true system model using the passive model discrimination algorithm, as described in the next subsection.

#### 4.3. Passive model discrimination

Using the computed optimal input and the observed measurements (corresponding to the unknown true model), the goal of passive model discrimination is to eliminate all models that are incompatible with the observed input-output trajectory at run time. We propose to achieve this goal (i.e., to solve Problem 2) by using a model invalidation approach to <code>invalidate/eliminate</code> each model that is inconsistent with the observed input-output trajectory, as described next:

**Theorem 2** (Model Invalidation). Given a discrete-time affine time-invariant model  $\mathcal{G}_i$ ,  $i \in \mathbb{Z}_N^+$ , and an input-output sequence  $\{u(k), z_m(k)\}_{k=0}^{T-1}$ , where u(k) is obtained from Theorem 1 and  $z_m(k)$  is observed at run time, the model  $\mathcal{G}_i$  is invalidated if the following problem is infeasible:

Find 
$$\underline{\mathbf{x}}_{i}(k), d_{i}(k), w_{i}(k), v_{i}(k), \gamma_{s}^{(j)}(k), \alpha^{(j)}(k), \gamma_{p}^{(t)}(k), \beta^{(t)}(k),$$

$$\forall k \in \mathbb{Z}_{T-1}^{0}, \forall j \in \mathbb{Z}_{n}^{+}, \forall t \in \mathbb{Z}_{n_{n}}^{+}$$

s.t.  $\forall k \in \mathbb{Z}_{T-1}^0, \forall j \in \mathbb{Z}_{n_s}^+, \forall t \in \mathbb{Z}_{n_n}^+$ :

$$\underline{\mathbf{x}}_{i}(k+1) = A_{i}\underline{\mathbf{x}}_{i}(k) + B_{i}\underline{\mathbf{u}}_{i}(k) + B_{w,i}w_{i}(k) + f_{i}, \tag{39a}$$

$$z_m(k) = C_i \underline{\mathbf{x}}_i(k) + D_i \underline{\mathbf{u}}_i(k) + D_{v,i} v_i(k) + g_i, \tag{39b}$$

$$P_{s,i}^{(j)}x_i(k) - p_{s,i}^{(j)} \le \alpha^{(j)}(k), \tag{39c}$$

$$\begin{bmatrix} Q_{ux,i}^{(t)} \\ P_{ux,i}^{(t)} \end{bmatrix} x_i(k) \le \begin{bmatrix} q_{u,i}^{(t)} - Q_{uu}^{(t)} u(k) \\ p_{ux,i}^{(t)} \end{bmatrix} + \beta^{(t)}(k), \tag{39d}$$

$$\gamma_s^{(j)}(k) \in \{0, 1\}, SOS-1:(\alpha^{(j)}(k), \gamma_s^{(j)}(k)), \sum_{j=1}^{n_s} \gamma_s^{(j)}(k) \ge 1,$$
 (39e)

$$\gamma_p^{(t)}(k) \in \{0, 1\}, SOS-1:(\beta^{(t)}(k), \gamma_p^{(t)}(k)), \sum_{j=1}^{n_p} \gamma_p^{(t)}(k) = 1,$$
 (39f)

$$w_i(k) \in \mathcal{W}_i, \ v_i(k) \in \mathcal{V}_i, \ d_i(k) \in \mathcal{D}_i,$$
 (39g)

$$\mathbf{x}_{i}^{0} \in \mathcal{X}_{0}, \ x_{i}(k) \in \mathcal{X}_{x,i}, \ y_{i}(k) \in \mathcal{X}_{y,i}, \tag{39h}$$

where  $\underline{\boldsymbol{x}}_i(k) = \begin{bmatrix} x_i(k) \\ y_i(k) \end{bmatrix}$  and  $\underline{\boldsymbol{u}}_i(k) \triangleq \begin{bmatrix} u(k) \\ d_i(k) \end{bmatrix}$ ,  $\alpha^{(j)}(k)$  and  $\beta^{(t)}(k)$  are slack variables that are free when  $\gamma_s^{(j)}(k)$  and  $\gamma_p^{(t)}(k)$  are zero, respectively. Otherwise,  $\alpha^{(j)}(k)$  and  $\beta^{(t)}(k)$  are zero due to the special ordered set of degree 1 (SOS-1) constraint (cf. Definition 1).

**Proof.** By leveraging Lemmas 2 and 3, the disjunctive constraint (12) and the coupled state–input constraint (13) can be constructed as (39c) with (39d) and (39e) with (39f), respectively. If the above optimization problem is infeasible, it means that the input–output sequence  $\{u(k), z_m(k)\}_{k=0}^{T-1}$  cannot be consistent with the model  $\mathcal{G}_i$ , hence the model is invalidated.  $\square$ 

Then, to solve the passive model discrimination problem in Problem 2, we can leverage the model invalidation approach in Theorem 2 to discard all inconsistent models. Here, the real-time *T*-length input-output trajectory can only be consistent with one model, since we applied the optimal discriminating input from Theorem 1. Hence, the true model can be identified once all other inconsistent models are eliminated, which is guaranteed by Theorem 1. This passive model discrimination (or model selection) process is summarized in the following Algorithm 1.

## **Algorithm 1:** Length-*T* Passive Model Discrimination

```
Data: Models \{\mathcal{G}_i\}_{i=1}^N, Input-Output Trajectory\{u(k), z_m(k)\}_{k=0}^{T-1}

1 function findModel (\{\mathcal{G}_i\}_{i=1}^N, \{u(k), z_m(k)\}_{k=0}^{T-1})

2 | valid \leftarrow \{\mathcal{G}_i\}_{i=1}^N;

3 | for i=1:N do

4 | Check Feasibility of Theorem 2;

5 | if infeasible then

6 | Remove i from valid;

7 | end

8 | end

9 | return valid
```

Table 1
Complexity of the AMD and MI algorithms.

	AMD	MI
No. of CV	$\mathcal{O}((c_0 + c_d + c_w + c_v + c_x + c_y + m_d + m_w + m_v + n_s c_s + n_p (c_{p1} + c_{p2}))TN^2)$	$(n_x + n_y + m_d + m_w + m_v + n_s c_s + n_p (c_{p1} + c_{p2}))T$
No. of IV	$\mathcal{O}((n_s + n_p)TN^2)$	2T
No. of SOS-1 constraints	$\mathcal{O}((c_0 + c_d + c_w + c_v + c_x + c_y + n_p + n_s)TN^2)$	$\frac{(n_s n_p (n_x + n_y) + n_s c_s + n_p (c_{p1} + c_{p2}) + c_0 + c_x + c_y + c_d + c_w + c_v)T}{c_x + c_y + c_d + c_w + c_v)T}$

#### 4.4. Computational complexity

Finally, we analyze the computational complexity of proposed active model discrimination and (AMD) and model invalidation (MI) algorithms in terms of the number of continuous variables (CV), integer variables (IV) and SOS-1 constraints, and they are given in Table 1, where the constants/parameters are defined in Section 3.2. From the table, it is clear that the AMD algorithm is more complex and requires more computational resources than MI, since the number of continuous variables, the number of integer variables and the number of SOS-1 constraints in AMD are of order  $TN^2$ , while the number of continuous variables, the number of integer variables and the number of SOS-1 constraints in the MI algorithm are of order T. It is noteworthy this is not a huge problem since the AMD algorithm is typically solved offline/at design time, while the MI algorithm is solved at run time.

### 5. Simulation examples

In this section, we apply our proposed approach to the motivating example of Section 2 and a permanent magnet DC motor example. In both examples, we solve the active model discrimination problem in Problem 1 offline to generate an optimal discriminating input, which is then implemented at run time and the resulting outputs/measurements are obtained. Using the collected input–output trajectory, we apply Algorithm 1 to identify the true model at run time. All the examples are implemented on a 1.3 GHz Dual-Core machine with 16 GB of memory. For the implementation of proposed approach, we utilized YALMIP [21] and Gurobi [19] in the MATLAB 2019b environment.

#### 5.1. Intention identification in an overtaking scenario

In this simulation example, we return to the motivating example in Section 2 of an overtaking scenario, where the ego car is initially behind the other car, and the other car has a constant lateral position  $y_o$ . We begin by describing the intention models in detail and then demonstrate that our approach is indeed able to identify the true intention model. In addition, we show that our approach outperforms an approach from [17] that leverages a sequence of restrictions, which we found to be also applicable in the presence of the disjunctive and coupled constraints.

## 5.1.1. Intention models

Two driver intentions  $i \in \{A, C\}$  for the other car, corresponding to Annoying and Cautious drivers are defined as:

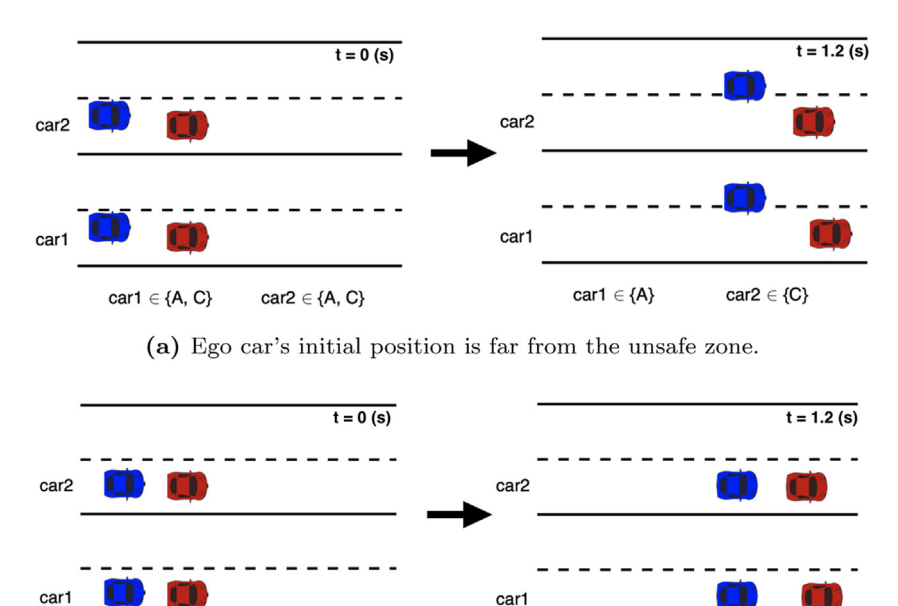
$$u_{x_0,i} = u_{x_0,0} + K_{i,1}\Delta y + K_{i,2}\Delta h_i + \delta_i, \tag{40}$$

where  $\Delta y = y_e - y_o$ ,  $\Delta h_A = h_{max} - h$  with  $h_{max}$  being the maximal distance where the other car notices the overtaking behavior of the ego car,  $\Delta h_C = h$ ,  $K_{i,1}$  and  $K_{i,2}$  are constants and  $\delta_i$  is an input uncertainty accounting for non-deterministic driving behavior.  $u_{xo,0} = -K_0(v_{xo} - v_{xo}^{\text{des}}) + C_d v_{xo}^{\text{des}}$  is a baseline controller that represents other car's default behavior to maintain a desired speed  $v_{xo}^{\text{des}}$ . In (40),  $K_{A,1} > 0$  and  $K_{A,2} > 0$  are chosen such that the annoying driver drives aggressively and speeds up to prevent being overtaken, while  $K_{C,1} < 0$  and  $K_{C,2} < 0$  for the cautious driver who slows down and makes it easier for the ego car to overtake. The specific parameter values in (40) are chosen as:  $K_{A,1} = 0.1$ ,  $K_{A,2} = 0.08$ ,  $\delta_A \in [-0.147, 0.147]$  (m/s²),  $K_{C,1} = -0.1$ ,  $K_{C,2} = -0.1$ ,  $\delta_C \in [-0.147, 0.147]$  (m/s²),  $K_0 = 0.1$ ,  $k_{min} = 6$  (m),  $k_{max} = 32$  (m),  $k_0 = 0.1$ ,  $k_0 =$ 

For the safety constraint (2) and the coupled state-input constraint (3), we chose  $w_{car}=1.8$  (m),  $y_{lane}=3.7$  (m),  $v_{xe}^{dz}=10$  (m/s), and  $\beta_1=\beta_2=1$ . The cost function is set as  $J(u_T)=\|u_T\|_2$ , and the time horizon is T=4 with a sampling time  $\delta_t=0.3$  (s). The ego car's longitudinal velocity and the other car's velocity are measured as the output, given by

$$z(k) = \begin{bmatrix} z_e(k) \\ z_o(k) \end{bmatrix} = \begin{bmatrix} v_{xe}(k) + v_e(k) \\ v_{xo}(k) + v_o(k) \end{bmatrix}$$

with  $v_e(k)$  and  $v_o(k)$  being the measurement noise signals. The process and measurement noise signals are limited to the range of [-0.01, 0.01]. Other parameters in the simulation are chosen as  $C_d = 0.15$  (1/s),  $v_{xe} \in [0, 34]$  (m/s),  $h \in [-32, 32]$  (m),  $y_e \in [0.9, 6.5]$  (m),  $v_{xo} \in [10, 28]$  (m/s),  $u_{xe} \in [-4.2, 4.2]$  (m/s<sup>2</sup>),  $v_{ye} \in [-2.5, 2.5]$  (m/s),  $v_{xo}^{des} = 22$  (m/s),  $v_{xo}^{des} = 22$  (m/s),  $v_{xo}^{des} = 22$  (m/s).



(b) Ego car's initial position is close to the unsafe zone.

 $car1 \in \{A\}$ 

 $car2 \in \{C\}$ 

**Fig. 2.** Intention estimation results when implementing the separating input obtained from the proposed active and passive model discrimination approaches for the overtaking scenario subject to different ego car's initial positions. The corresponding animation can be found at https://youtu.be/BlboF40m4D8.

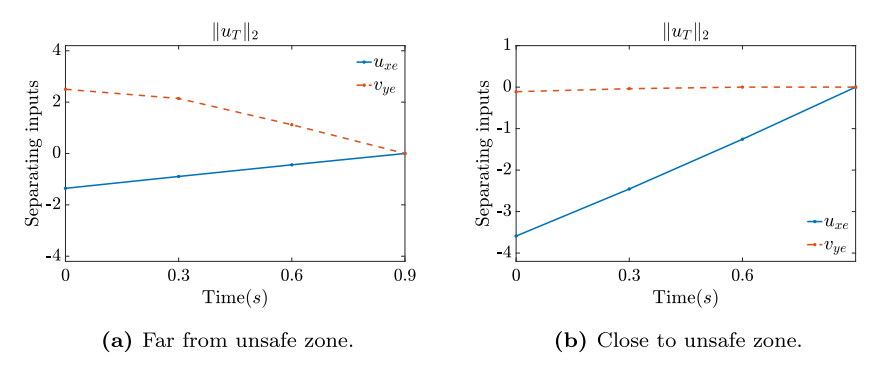


Fig. 3. Optimal inputs obtained by solving the proposed active model discrimination under different initial ego car positions.

## 5.1.2. Intention estimation with different initial ego car positions

car1 ∈ {A, C}

 $car2 \in \{A, C\}$ 

In the following, we consider the intention estimation/identification problem using our proposed model discrimination approach for two different cases, which is also used in the following subsection when we compare our approach and [17] that leverages sequence of restrictions for tackling the coupled state-input constraints.

In the first case, the initial conditions of the ego car and the other car are  $v_{xe}(0) \in [22, 26]$  (m/s),  $v_e(0) \in [2, 2.8]$  (m),  $h(0) \in [10, 20]$  (m),  $v_{xo}(0) \in [21, 23]$  (m/s). As seen in Fig. 2(a), the other car 1 is Annoying and attempts to speed up so that the ego car cannot overtake it, while the other car 2 is Cautious and slows down slightly to let the ego car overtake it. Since the ego car's initial position is far from the unsafe zone, the computed discriminating/separating inputs (cf. Fig. 3(a)) led the ego car to perform overtaking. Furthermore, although our approach is based on an implicit representation of the reachable sets of the system, for the sake of illustration, we explicitly compute the reachable output sets by using the MPT toolbox [22] at each time instance under the optimal discriminating/separating input, as depicted in Fig. 4, where the two intentions are completely separated at k = 4 despite the considered uncertainties, noise signals and constraints.

In the second case, the ego car's initial position is close to the unsafe zone. The initial conditions are  $v_{xe}(0) \in [22, 26]$  (m/s),  $v_{e}(0) \in [1.85, 2.8]$  (m),  $v_{e}(0) \in [9, 12]$  (m),  $v_{e}(0) \in [21, 23]$  (m/s). Similar to the first scenario, the computed separating inputs discriminate the other car's intention successfully. However, as observed in Fig. 2(b), the

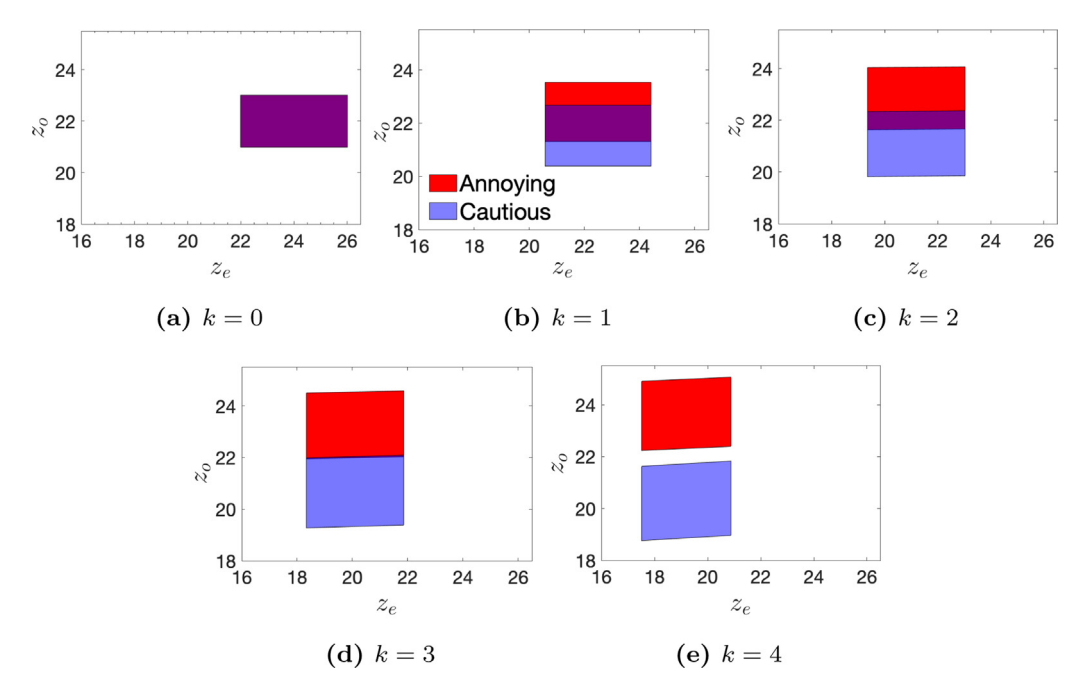


**Fig. 4.** Reachable output sets given the optimal separating input at k = 0, ..., 4 in the case that the ego car's initial position is far away from the unsafe zone. The dark purple area is the overlap of the reachable output sets of the two models. (For interpretation of the references to color in this figure legend, the reader is referred to the web version of this article.)

ego car does not overtake the other car while estimating other car's intention. Since the initial position of the ego car is close to the unsafe zone, the ego car has to slow down (cf. Fig. 3(b)) to satisfy the safety constraint  $h > h_{min}$ . Meanwhile, this action already reveals the intention of the other driver without performing an overtake. In addition, for illustration purposes, the reachable output sets under the computed optimal discriminating/separating input in the case that the ego car's initial position is close to the unsafe zone are also shown in Fig. 5, from which we observe that the two intentions can be separated at k=3.

## 5.1.3. Comparisons with the approach leveraging a sequence of restrictions

We also compared our approach based on Equivalence (ii) of Lemma 1 with the approach leveraging a sequence of restrictions from [17] in the overtaking scenario subject to the initial conditions in both of the cases above. Specifically, a sequence of restrictions is only applied to the controlled state constraints, resulting in a sequence of MIQPs, while safety constraints and separation conditions are still handled by using the KKT-based approach in Equivalence (ii) of Lemma 1. The approach in [17] required a CPU time of 54.69 (s) and 53.37 (s) (2 iterations) for the two cases, while our approach only needed 37.96 (s) and 38.39 (s) to achieve the same cost. This demonstrates that the proposed approach required almost 30% less computational time to find the optimal solution in both cases. Moreover, when increasing the input uncertainty level in intention model (40) from  $\delta_A$ ,  $\delta_C \in [-0.147, 0.147]$  (m/s²) to  $\delta_A$ ,  $\delta_C \in [-0.210, 0.210]$  (m/s²) in the first case, the method in [17] led to an infeasible solution, while our approach was able to obtain the optimal input with a CPU time of 38.49 (s).

Further, to test the effectiveness of our approach with more possible models, we also consider another intention model called Inattentive i=I, which means the inattentive driver/behavior fails to notice the ego vehicle and tries to maintain the desired velocity. The inattentive intention is modeled by setting  $K_{I,1}=0$  and  $K_{I,2}=0$  in Eq. (40). We consider the active model discrimination problem with the input uncertainty level  $\delta_A$ ,  $\delta_C \in [-0.147, 0.147]$  and the case, ego car's initial position is close to the unsafe zone. In this case with three intent models, our proposed approach is able to a feasible separating input that can separate the models within T=8, i.e.,  $\{u_{x,e}\}_T=\{-4.200, -4.200, -4.200, -4.200, 3.1324, 4.200, -4.200, -4.200\}$  and  $\{v_{y,e}\}_T=\{2.500, 2.500, 2.500, -2.500, -2.500, 2.500, -2.500, -2.500, -2.500, -2.500, -2.500, 2.500, -2.50$ 

Based on these observations, we can conclude that our approach outperforms [17] in terms of completeness, optimality and computational performance.

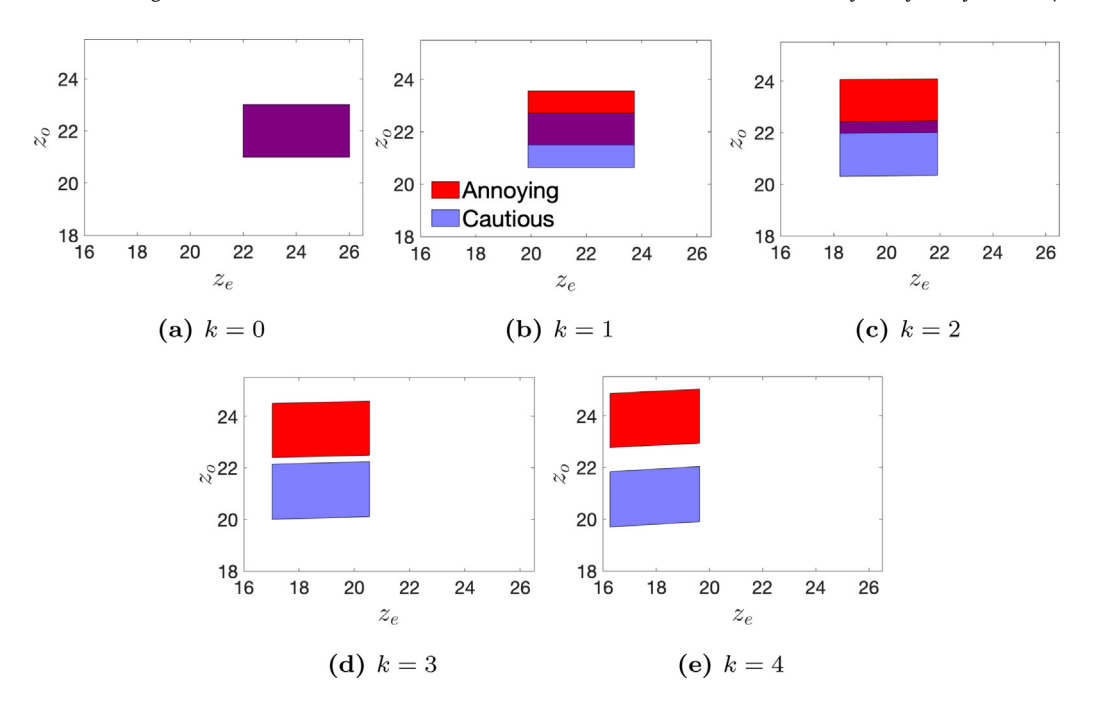


**Fig. 5.** Reachable output sets given the optimal separating input at  $k = 0, \dots, 4$  in the case that the ego car's initial position is close to the unsafe zone. The dark purple area is the overlap of the reachable output sets of the two models. (For interpretation of the references to color in this figure legend, the reader is referred to the web version of this article.)

**Table 2** Fault model parameters.

Model	$R_a(\Omega)$	$L (10^{-3} \text{ H})$	$K_e \ (10^{-2} \ \frac{\text{Vrad}}{\text{s}})$	$J_1 \ (10^{-4} \ \frac{\rm Js^2}{\rm rad})$	$f_r \ (10^{-4} \ \frac{\rm Js}{\rm rad})$
1	1.2030	5.5840	8.1876	1.3528	2.3396
2	1.7725	5.5837	8.0203	1.3320	2.3769
3	1.7690	6.0798	8.7987	1.4964	2.3570

#### 5.2. Permanent magnet DC motor

We further apply our proposed model discrimination approach to fault detection/identification of DC motors, based on an example in [11]. The time-discretized dynamics of a permanent magnet DC motor is described in [11,23] and given by

$$i(k+1) = \left(1 - \frac{R_a}{L}\delta t\right)i(k) - \left(\frac{K_e}{L}\delta t\right)\omega(k) + \left(\frac{1}{L}\delta t\right)u(k),$$

$$\omega(k+1) = \left(\frac{K_t}{J}\delta t\right)i(k) + \left(1 - \frac{f_r}{J_1}\delta t\right)\omega(k) + \left(\frac{1}{J_1}\delta t\right)\tau_c(k),$$
(41)

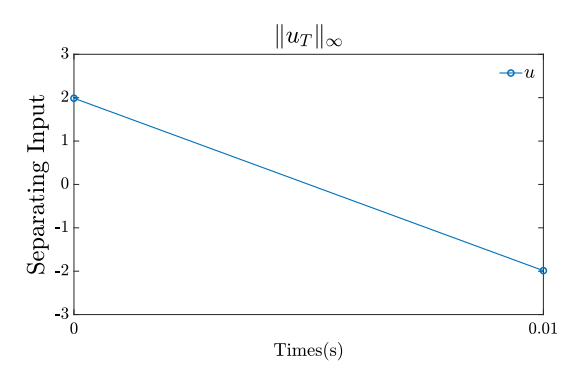
where u is the armature voltage, i is the current,  $\omega$  is the angular velocity of the rotor,  $\tau_c$  is the Coulomb friction,  $R_a$  is the resistance, L is the inductance,  $K_e$  is torque constant,  $K_t = 1.0005K_e$  is the back EMF constant,  $K_t = 1.0005K_e$  is the viscous friction coefficient, and  $K_t = 1.0005K_e$  is the viscous friction coefficient, and  $K_t = 1.0005K_e$  is the viscous friction coefficient, and  $K_t = 1.0005K_e$  is the viscous friction coefficient, and  $K_t = 1.0005K_e$  is the viscous friction coefficient, and  $K_t = 1.0005K_e$  is the viscous friction coefficient, and  $K_t = 1.0005K_e$  is the viscous friction coefficient, and  $K_t = 1.0005K_e$  is the viscous friction coefficient, and  $K_t = 1.0005K_e$  is the viscous friction coefficient, and  $K_t = 1.0005K_e$  is the viscous friction coefficient, and  $K_t = 1.0005K_e$  is the viscous friction coefficient, and  $K_t = 1.0005K_e$  is the viscous friction coefficient, and  $K_t = 1.0005K_e$  is the viscous friction coefficient, and  $K_t = 1.0005K_e$  is the viscous friction coefficient, and  $K_t = 1.0005K_e$  is the viscous friction coefficient, and  $K_t = 1.0005K_e$  is the viscous friction coefficient.

Note that in comparison to [11,23], we consider a slightly more realistic DC motor model with a dead-zone and a Coulomb friction term that is known to be nonlinear [24]. In particular, based on [24], we consider the value of the Coulomb friction to be state-dependent as follows (for all k):

$$\tau_c(k) = \begin{cases} \alpha_1, & \text{if } \omega(k) \le 0, \\ \alpha_2, & \text{if } \omega(k) \ge 0, \end{cases}$$
(42)

and additionally, we consider a symmetric dead-zone threshold  $\omega^{dz}$  (where the rotor does not rotate) and to ensure that the rotor does not stop, we impose a disjunctive constraint (cf. (12)) that the angular velocity  $\omega(k)$  must satisfy:

$$\{\omega(k) < -\omega^{dz}\} \vee \{\omega(k) > \omega^{dz}\}, \quad \text{(for all } k > 1).$$



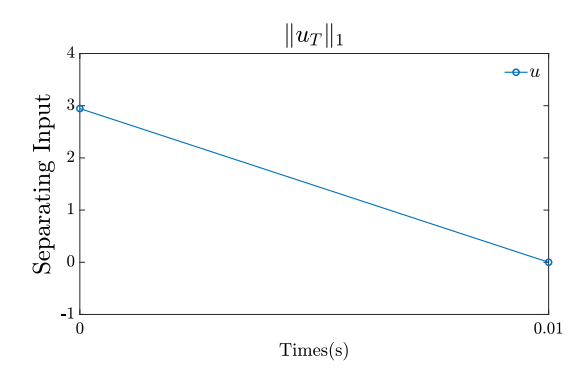


Fig. 6. Optimal input obtained by solving the proposed active model discrimination under different cost functions.

As described in Table 2, three models are considered based on the model parameters in Table 2 of [11]. Model 1 is fault-free, while the fault model 2 is due to the increase of armature resistance by +0.5 ( $\Omega$ ) and the fault model 3 is due to the wearing of the brush, leading to insufficient brush pressure.

The initial conditions are assumed to satisfy  $i(0) \in [0.54, 0.66]$  (A) and  $\omega(0) \in [0.02, 0.07]$  (rad/s) and we consider  $\omega^{dz} = 0.1$  (rad/s). Since our initial rotor angular velocity is set in the dead zone and is positive,  $\tau_c(0) = \alpha_2$ . Moreover, the current is constrained by  $i(k) \in [-10, 10]$  (A) and the rotor angular velocity is constrained by  $\omega(k) \in [-150, 150]$  (rad/s) for all  $k \in \mathbb{Z}_T^+$ , while the input armature voltage is bounded by  $u(k) \in [-12, 12]$  (V). The other parameters are chosen as  $\epsilon = 0.0001$ ,  $\alpha_1 = 0.001$ , and  $\alpha_2 = -0.005$ . Moreover, we consider two cost functions, i.e.,  $J(u_T) = \|u_T\|_{\infty}$  and  $J(u_T) = \|u_T\|_1$  with  $u_T = \{u(k)\}_{k=0}^{T-1}$ , and the time horizon is T = 2 with a sampling time  $\delta_t = 0.005$  (s).

In order to account for parameter uncertainties, similar to [11], the state dynamics in (41) were augmented with the term  $B_{w,i}w(k)$ , where

$$B_{w,1} = \begin{bmatrix} -0.0254 & -0.0778 \\ -0.3996 & 0.3026 \end{bmatrix}, B_{w,2} = \begin{bmatrix} -0.0231 & -0.0471 \\ -0.3470 & 0.2798 \end{bmatrix}, B_{w,3} = \begin{bmatrix} -0.0242 & -0.0537 \\ -0.3516 & 0.2797 \end{bmatrix},$$

and the process noise is limited by  $w(k) \in \mathcal{W} = \{w : \|w\|_{\infty} \le 1\}$ . The current and rotor angular velocity are measured as the output, given by

$$y(k) = \begin{bmatrix} i(k) + \nu_i(k) \\ \omega(k) + \nu_{\omega}(k) \end{bmatrix}$$

with  $v_i(k)$  and  $v_\omega(k)$  being the measurement noises, both being limited to the range of [-0.06, 0.06]. Fig. 6 shows the separating inputs computed in Theorem 1 that can successfully discriminate the fault models at T=2 with different cost functions. Similar to the intention estimation example, for the sake of illustration, we also explicitly depict the output reachable sets for the case with  $J(u_T) = \|u_T\|_\infty$  in Fig. 7 by using the MPT toolbox [22] to verify the effectiveness of the computed separating input. Further, to demonstrate that our approach can scale to problems with more models, we increased the number of the fault models to 5 with the parameters for the two additional models corresponding to Models 5 and 6 in [11]. Our simulation results show that our proposed approach can obtain a separating input for discriminating among all five fault modes within T=2, although this result is sub-optimal given that we terminated the optimization problem on our limited simulation platform after 2 days.

Furthermore, we also applied our proposed method to the fault detection example of DC motors in [11] that does not consider the velocity dead-zone and the Coulomb friction, and specifically, we considered models 1, 2, 4 and 6. The optimal separating input is shown in Fig. 8, and the corresponding output reachable sets are depicted in Fig. 9. It is clear from Fig. 9 that our proposed method can successfully separate fault models within 2 time steps.

#### 6. Conclusion

In this paper, we considered the active and passive model discrimination problems among a finite number of models subject to disjunctive and coupled constraints. These general constraints can be used to represent state-dependent piecewise input constraints, e.g., curvature constraints or input saturation, and disjunctive state constraints, e.g., non-convex safety restrictions or collision-free regions. We proposed to reformulate these constraints by leveraging KKT conditions and introducing binary variables, thus converting the model discrimination problems into tractable MILP/MIQP problems. Finally, we illustrated the effectiveness of the proposed approach with simulation examples for identifying driver intention in an overtaking scenario and for discriminating/identifying fault in an example with a permanent magnetic DC motor. Future works would include the consideration of piecewise intention models in the context of passive and active model discrimination. In addition, how to further reduce the computational complexity of our proposed model discrimination approach to make it applicable to examples with a high number of models is also an interesting future direction.

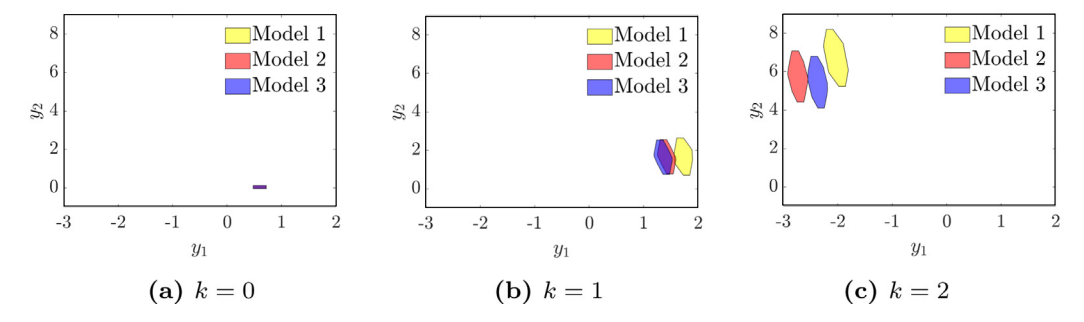


**Fig. 7.** Reachable output sets given the optimal separating input at k = 0, 1, 2 for the case with  $J(u_T) = ||u_T||_{\infty}$ . The dark blue area is the overlap of the reachable output sets of the three models. (For interpretation of the references to color in this figure legend, the reader is referred to the web version of this article.)

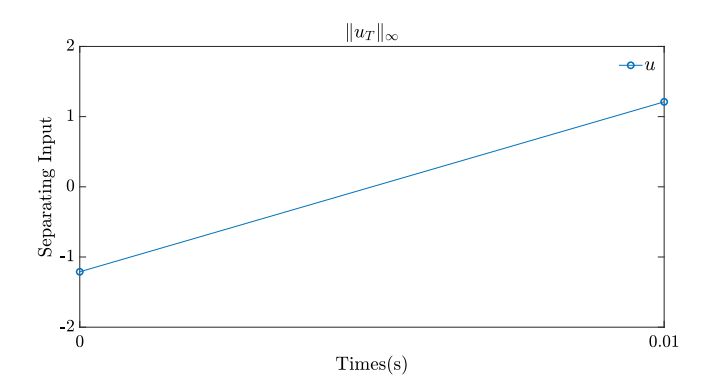


Fig. 8. Optimal input obtained by solving the proposed active model discrimination for the DC motor example in [11].

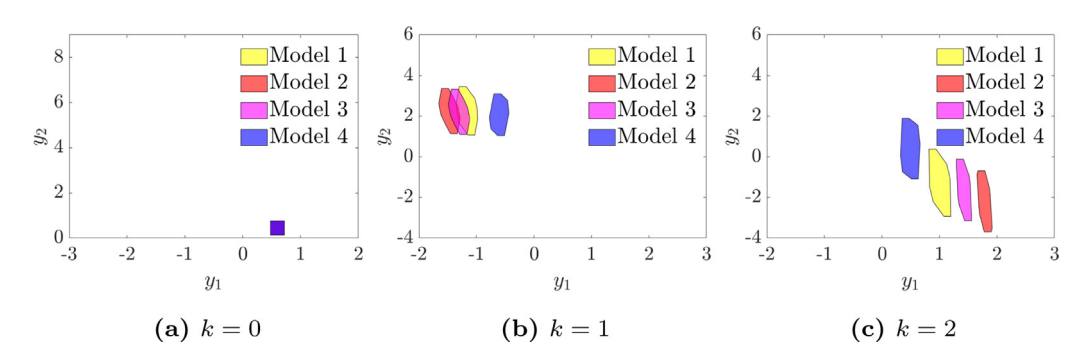


Fig. 9. Reachable output sets given the optimal separating input at k = 0, 1, 2 for the case with  $J(u_T) = ||u_T||_{\infty}$  for the DC motor example in [11].

#### **CRediT authorship contribution statement**

**Qiang Shen:** Conceptualization, Methodology, Investigation, Software, Writing – original draft, Writing – review & editing. **Ruochen Niu:** Investigation, Validation, Software, Writing – original draft, Writing – review & editing. **Sze Zheng Yong:** Supervision, Conceptualization, Methodology, Writing – original draft, Writing – review & editing.

## **Declaration of competing interest**

The authors declare that they have no known competing financial interests or personal relationships that could have appeared to influence the work reported in this paper.

## Acknowledgments

This work is partially supported by the Defense Advanced Research Projects Agency (DARPA), USA grant D18AP00073, the National Science Foundation, USA grants CNS-1943545 and CNS-1932066, the National Natural Science Foundation of

China grants U20B2054 and 62103275, the Natural Science Foundation of Shanghai, China grant 20ZR1427000 and the Shanghai Sailing Program, China grant 20YF1421600.

## Appendix A. Matrices and vectors pair-concatenated dynamics in (17)-(20)

The pair-concatenated dynamics in (17)–(20) can be obtained in two steps. In the first step, we concatenate the states and outputs in (7) and (8) over the time horizon T, and re-write the time-concatenated model in terms of the uncertain variables including the time-stacked initial state  $\mathbf{x}_0$ , input vectors  $u_T$ ,  $d_T$ , and noise  $w_T$ ,  $v_T$ , as follows:

$$\mathbf{x}_{i,T} = M_{x,i,T} \mathbf{x}_{i}^{0} + \Gamma_{xu,i,T} u_{T} + \Gamma_{xd,i,T} d_{i,T} + \Gamma_{xw,i,T} w_{i,T} + \tilde{f}_{x,i,T}, \tag{A.1}$$

$$y_{i,T} = M_{v,i,T} \mathbf{x}_i^0 + \Gamma_{vu,i,T} u_T + \Gamma_{vd,i,T} d_{i,T} + \Gamma_{vw,i,T} w_{i,T} + \tilde{f}_{v,i,T}, \tag{A.2}$$

$$\underline{\mathbf{x}}_{i,T} = \bar{A}_{i,T} \underline{\mathbf{x}}_{i}^{0} + \Gamma_{u,i,T} u_{T} + \Gamma_{d,i,T} d_{i,T} + \Gamma_{w,i,T} w_{i,T} + \tilde{f}_{i,T}, \tag{A.3}$$

$$z_{i,T} = E_i \mathbf{x}_i^0 + F_{u,i} u_T + F_{d,i} d_{i,T} + F_{u,i} v_{i,T} + \tilde{g}_{i,T}. \tag{A.4}$$

To obtain the above, we first define the operator  $\Theta_{i,T}(\Omega) = \begin{bmatrix} \Omega & 0 & \cdots & 0 \\ A_i \Omega & \Omega & \cdots & 0 \\ \vdots & \vdots & \ddots & \vdots \\ A_i^{T-1} \Omega & A_i^{T-2} \Omega & \cdots & \Omega \end{bmatrix}$ , as well as  $\overline{A}_{i,T} = \begin{bmatrix} A_i \\ A_i^2 \\ \vdots \\ A_i^{T-1} \end{bmatrix}$ ,  $\dagger = \{x, y\}$  and  $\star = \{u, d, w\}$ . The involved matrices and vectors in (A.1)–(A.4) can then be constructed as follows:

1. In (A.1)-(A.2), 
$$M_{\dagger,i,T} = A_{\dagger,d,i,T} \begin{bmatrix} \mathbb{I} \\ \overline{A}_{i,T-1} \end{bmatrix}$$
 with  $A_{\dagger,d,i,T} = \operatorname{diag}_{T} \{ \begin{bmatrix} A_{\dagger x,i} & A_{\dagger y,i} \end{bmatrix} \}$ ;

2. In (A.1)-(A.2), 
$$\Gamma_{\uparrow\star,i,T} = A_{\uparrow,d,i,T} \begin{bmatrix} 0 & 0 \\ \Gamma_{\star,i,T-1} & 0 \end{bmatrix} + B_{\uparrow\star,d,i,T}$$
 with  $\Gamma_{\star,i,T-1} = \Theta_{i,T-1} \begin{pmatrix} B_{x\star,i} \\ B_{y\star,i} \end{pmatrix}$  and  $B_{\uparrow\star,d,i,T} = \operatorname{diag}_T \{B_{\uparrow\star,i}\};$ 

3. In (A.1)-(A.2), 
$$\tilde{f}_{\dagger,i,T} = A_{\dagger,d,i,T} \begin{bmatrix} 0 \\ \tilde{f}_{i,T-1} \end{bmatrix} + \overline{f}_{\dagger,i,T}$$
 with  $\tilde{f}_{i,T-1} = \Theta_{i,T-1}(\mathbb{I})\overline{f}_{i,T-1}$ ,  $\overline{f}_{i,T-1} = \operatorname{vec}_{T-1}\{f_i\}$  and  $\overline{f}_{\dagger,i,T} = \operatorname{vec}_{T}\{f_{\dagger,i}\}$ ;  
4. In (A.3),  $\Gamma_{\star,i,T} = \Theta_{i,T} \begin{bmatrix} B_{x\star,i} \\ B_{y\star,i} \end{bmatrix}$ ,  $\tilde{f}_{i,T} = \Theta_{i,T}(\mathbb{I})\overline{f}_{i,T}$  with  $\overline{f}_{i,T} = \operatorname{vec}_{T}\{f_i\}$ ;

4. In (A.3), 
$$\Gamma_{\star,i,T} = \Theta_{i,T} \left( \begin{bmatrix} B_{\mathsf{X}\star,i} \\ B_{\mathsf{V}\star,i} \end{bmatrix} \right)$$
,  $\tilde{f}_{i,T} = \Theta_{i,T}(\mathbb{I})\bar{f}_{i,T}$  with  $\bar{f}_{i,T} = \mathrm{vec}_T\{f_i\}$ 

5. In (A.4), 
$$E_i = \text{diag}_T\{C_i\}, F_{\star,i} = \text{vec}_T\{D_{\star,i}\}, \tilde{g}_{i,T} = \text{vec}_T\{g_i\}.$$

Next, in the second step, building upon the time-concatenated dynamics (A.1)-(A.4) from the first step, we further concatenate the time-concatenated dynamics for each model pair  $\iota = (\mathcal{G}_i, \mathcal{G}_j), \ \forall i, j \in \mathbb{Z}_N^+$  with  $i \neq j$ . Let  $\dagger = \{x, y\}$ and  $\star = \{u, d, w\}$ . For pair  $\iota = (\mathcal{G}_i, \mathcal{G}_i)$ , the matrices and vectors in the pair-concatenated dynamics (17)–(20) can be constructed as follows:

1. 
$$\ln (17)$$
– $(18)$ ,  $M_{\dagger}^{\iota} = \operatorname{diag}_{k=\{i,j\}}\{M_{\dagger,k,T}\}$ ,  $\Gamma_{\dagger u}^{\iota} = \operatorname{vec}_{k=\{i,j\}}\{\Gamma_{\dagger u,k,T}\}$ ,  $\Gamma_{\dagger d}^{\iota} = \operatorname{diag}_{k=\{i,j\}}\{\Gamma_{\dagger d,k,T}\}$ ,  $\Gamma_{\dagger w}^{\iota} = \operatorname{diag}_{k=\{i,j\}}\{\Gamma_{\dagger w,k,T}\}$ ,  $\tilde{f}_{\dagger}^{\iota} = \operatorname{vec}_{k=\{i,j\}}\{\tilde{f}_{\dagger,k,T}\}$ ;

2.  $\ln (19)$ ,  $\tilde{A}^{\iota} = \operatorname{diag}_{k=\{i,j\}}\{\tilde{A}_{k,T}\}$ ,  $\Gamma_{u}^{\iota} = \operatorname{vec}_{k=\{i,j\}}\{\Gamma_{u,k,T}\}$ ,  $\Gamma_{d}^{\iota} = \operatorname{diag}_{k=\{i,j\}}\{\Gamma_{d,k,T}\}$ ,  $\Gamma_{w}^{\iota} = \operatorname{diag}_{k=\{i,j\}}\{\Gamma_{w,k,T}\}$ ,  $\tilde{f}^{\iota} = \operatorname{diag}_{k=\{i,j\}}\{\Gamma_{w,k,T}\}$ 

2. 
$$\ln (19)$$
,  $\overline{A}^{\iota} = \operatorname{diag}_{k=\{i,j\}}\{\overline{A}_{k,T}\}$ ,  $\Gamma^{\iota}_{u} = \operatorname{vec}_{k=\{i,j\}}\{\Gamma_{u,k,T}\}$ ,  $\Gamma^{\iota}_{d} = \operatorname{diag}_{k=\{i,j\}}\{\Gamma_{d,k,T}\}$ ,  $\Gamma^{\iota}_{w} = \operatorname{diag}_{k=\{i,j\}}\{\Gamma_{w,k,T}\}$ ,  $\tilde{f}^{\iota} = \operatorname{vec}_{k=\{i,j\}}\{\tilde{f}_{k,T}\}$ ;

$$\begin{aligned} &\text{vec}_{k=\{i,j\}}\{\tilde{f}_{k,T}\};\\ &\text{3. In (20), } \overline{C}^t = \text{diag}_{k=\{i,j\}}\{E_k\}, \ \overline{D}^t_u = \text{vec}_{k=\{i,j\}}\{F_{u,k}\}, \ \overline{D}^t_d = \text{diag}_{k=\{i,j\}}\{F_{d,k}\}, \ \overline{D}^t_v = \text{diag}_{k=\{i,j\}}\{F_{v,k}\}, \ \tilde{g}^t = \text{vec}_{k=\{i,j\}}\{\tilde{g}_{k,T}\}. \end{aligned}$$

## Appendix B. Matrices and vectors in (21)

Similar to Appendix A, the matrices and vectors of the pair-concatenated state constraints and uncertainty constraints defined in (21) can also be obtained in two steps. Let  $\dagger = \{x, y\}$  and  $\star = \{u, d, w\}$ . In the first step, the state constraints (i.e., (10) and (11)) and uncertainty constraints (i.e., (14), (15) and (16)) of model  $\mathcal{G}_i$  over a time horizon of T are stacked/concatenated as follows:

$$H_{\uparrow,i,T}\bar{x}_{i,T} \leq \bar{p}_{\uparrow,i,T} - \bar{P}_{\uparrow,i,T}\tilde{f}_{\uparrow,i,T} - \bar{P}_{\uparrow,i,T}\Gamma_{\uparrow u,i,T}u_{T}, \quad H_{\bar{x},i,T}\bar{x} \leq h_{\bar{x},i,T}, \tag{B.1}$$

where the time-concatenated uncertainties are denoted as  $\bar{x}_{i,T} = [\underline{\boldsymbol{x}}_{i}^{0,T} \ d_{i,T}^{\mathsf{T}} \ v_{i,T}^{\mathsf{T}} \ v_{i,T}^{\mathsf{T}}]^{\mathsf{T}}, \ \bar{P}_{\uparrow,i,T} = \mathrm{diag}_{T}\{P_{\uparrow,i}\}, \ \bar{p}_{\uparrow,i,T} = \mathrm{vec}_{T}\{p_{\uparrow,i}\}, \ H_{\uparrow,i,T} = \bar{P}_{\uparrow,i,T} \left[M_{\uparrow,i,T} \ \Gamma_{\uparrow d,i,T} \ \Gamma_{\uparrow w,i,T} \ 0\right], \ H_{\bar{x},i,T} = \mathrm{vec}\{P_{0}, \bar{Q}_{d,i,T}, \bar{Q}_{w,i,T}, \bar{Q}_{v,i,T}\} \ \text{with} \ \bar{Q}_{\star,i,T} = \mathrm{diag}_{T}\{Q_{\star,i}\}, \ h_{\bar{x},i,T} = \mathrm{vec}\{p_{0}, \bar{q}_{d,i,T}, \bar{q}_{w,i,T}, \bar{q}_{v,i,T}\} \ \text{with} \ \bar{q}_{\star,i,T} = \mathrm{vec}_{T}\{q_{\star,k}\}.$ 

Then, in the second step, stacking the time-concatenated state and uncertainty constraints (B.1) for each model pair  $\iota = (\mathcal{G}_i, \mathcal{G}_j), \forall i, j \in \mathbb{Z}_N^+$  with  $i \neq j$ , we obtain the pair-concatenated state and uncertainty constraints in terms of uncertain variables for each model pair  $\iota$  (cf.  $\vec{x}^{\iota} = [\underline{x}_{0}^{\iota T} \ d_{T}^{\iota T} \ w_{T}^{\iota T}]^{\mathsf{T}}$ ), i.e., (21), where the involved matrices and vectors can be

constructed as follows:

$$\begin{split} \bar{P}_{\dagger}^{\iota} &= \underset{k = \{i,j\}}{\text{diag}} \{\bar{P}_{\uparrow,k,T}\}, \; \bar{p}_{\dagger}^{\iota} = \underset{k = \{i,j\}}{\text{vec}} \{\bar{p}_{\uparrow,k,T}\}, \; H_{\uparrow}^{\iota} = \bar{P}_{\uparrow}^{\iota} \left[ M_{\uparrow}^{\iota} \quad \Gamma_{\uparrow d}^{\iota} \quad \Gamma_{\uparrow w}^{\iota} \quad \mathbf{0} \right], \\ H_{\bar{\chi}}^{\iota} &= \text{diag} \{\bar{P}_{0}^{\iota}, \; \bar{Q}_{d}^{\iota}, \; \bar{Q}_{w}^{\iota}, \; \bar{Q}_{v}^{\iota}\} \; \text{with} \; \bar{P}_{0}^{\iota} = \underset{2}{\text{diag}} \{P_{0}\} \; \text{and} \; \bar{Q}_{\star}^{\iota} = \underset{k = \{i,j\}}{\text{diag}} \{Q_{\star,k,T}\}, \\ h_{\bar{\chi}}^{\iota} &= \text{vec} \{\bar{p}_{0}^{\iota}, \; \bar{q}_{d}^{\iota}, \; \bar{q}_{w}^{\iota}, \; \bar{q}_{v}^{\iota}\} \; \text{with} \; \bar{p}_{0}^{\iota} = \underset{2}{\text{vec}} \{p_{0}\} \; \text{and} \; \bar{q}_{\star}^{\iota} = \underset{k = \{i,j\}}{\text{vec}} \{q_{\star,k,T}\}. \end{split}$$

### Appendix C. Matrices and vectors in Proposition 4

$$\begin{split} & \text{For } * = \{d, \, v\} : \overline{F}^{\iota}_{*} = \begin{bmatrix} F_{*,i} & -F_{*,j} \\ -F_{*,i} & F_{*,j} \end{bmatrix} . \, \overline{E}^{\iota} = \begin{bmatrix} E_{i} & -E_{j} \\ -E_{i} & E_{j} \end{bmatrix}, \\ & \Lambda^{\iota} = \overline{E}^{\iota} \left[ \overline{A}^{\iota} & \Gamma^{\iota}_{d} & \Gamma^{\iota}_{w} & \mathbf{0} \right] + \begin{bmatrix} \mathbf{0} & \overline{F}^{\iota}_{d} & \mathbf{0} & \overline{F}^{\iota}_{v} \end{bmatrix}. \\ & \text{For } \dagger = \{x, y\} : \Gamma^{\iota}_{\dagger u} = \underset{k = \{i, j\}}{\text{vec}} \{\Gamma_{\dagger u, k, T}\}, \, \Gamma^{\iota}_{\dagger d} = \underset{k = \{i, j\}}{\text{diag}} \{\Gamma_{\dagger d, k, T}\}, \\ & \Gamma^{\iota}_{\dagger w} = \underset{k = \{i, j\}}{\text{diag}} \{\Gamma_{\dagger w, k, T}\}, \, M^{\iota}_{\dagger} = \underset{k = \{i, j\}}{\text{diag}} \{M_{\dagger, k, T}\}, \, \tilde{f}^{\iota}_{\dagger} = \underset{k = \{i, j\}}{\text{vec}} \{\tilde{f}_{\dagger, k, T}\}. \\ & \overline{F}^{\iota}_{u} = \begin{bmatrix} F_{u, i} - F_{u, j} \\ F_{u, j} - F_{u, i} \end{bmatrix}, \, \overline{g}^{\iota} = \begin{bmatrix} \tilde{g}_{i} - \tilde{g}_{j} \\ -\tilde{g}_{i} + \tilde{g}_{j} \end{bmatrix}, \, R^{\iota} = \begin{bmatrix} H^{\iota}_{y} \\ \Lambda^{\iota} \end{bmatrix}, \\ & r^{\iota} = \begin{bmatrix} \overline{p}^{\iota}_{y} - \overline{p}^{\iota}_{y} \tilde{f}^{\iota}_{y} \\ -\overline{E}^{\iota} \tilde{f}^{\iota} \end{bmatrix}, \, S^{\iota} = \begin{bmatrix} \overline{P}^{\iota}_{y} \Gamma^{\iota}_{y u} \\ \overline{E}^{\iota} \Gamma^{\iota}_{u} + F^{\iota}_{u} \end{bmatrix}. \end{split}$$

## Appendix D. Proof of Lemma 1

The generalized semi-infinite constraint in (29) can be viewed as introducing a bilevel structure [18] and is equivalent to  $\max_{\chi \in \mathcal{X}(y)} p \leq 0$ , where  $p \triangleq \mathcal{A}\chi - b - \mathcal{C}y$ , and  $\mathcal{X}(y) \triangleq \{\chi : \mathcal{D}\chi \leq e + \mathcal{F}y, \, \mathcal{G}\chi \leq h\}$ . Using this, Equivalence (i) can be obtained as the robust counterpart of the lower level problem using duality tools from robust optimization [25,26]. On the other hand, to obtain Equivalence (ii), since each row of p must be maximized, we introduce a slack variable  $p_a$  for each row and convert the semi-infinite constraint into finitely many linear constraints  $p_a^* \leq 0$ , where  $p_a^*$  is the maximum  $p_a$  satisfying constraints in  $\mathcal{X}$ , i.e.,

$$\begin{split} p_a^* &= \arg\min_{p_a, \mathcal{X}_a} - p_a \\ \text{s.t.} \quad \mathcal{D} \chi_a &\leq e + \mathcal{F} y, \ \mathcal{G} \chi_a \leq h, \ \ p_a = \mathcal{A}_{(a)} \chi_a - b_{(a)} - \mathcal{C}_{(a)} y. \end{split}$$

Then, applying KKT conditions and rewriting the complementary slackness constraints as SOS-1 constraints, we obtain Equivalence (ii).  $\Box$ 

### Appendix E. Proof of Lemma 2

By introducing the binary variables  $r^{(i)}$  and slack variables  $s^{(i)}$ , by the definition of SOS-1 constraints, the constraint (32b) guarantees that at least one  $r^{(i)}$  must be 1, thus, at least one  $s^{(i)}$  must be zero, i.e.,  $q^{(i)} \le s^{(i)} = 0$ .

## Appendix F. Proof of Lemma 3

The binary variable  $\gamma^{(i)}=1$  implies that  $\mathcal{S}^{(i)}\chi+\mathcal{T}^{(i)}y\leq\beta^{(i)}$  holds and by the piecewise constraint,  $Q^{(i)}\chi+\mathcal{R}^{(i)}y\leq\alpha^{(i)}$  holds, while the SOS-1 constraint ensures that  $t^{(i)}=0$ . Combining them, we have (33a) with  $t^{(i)}=0$ . Otherwise,  $\gamma^{(i)}=0$  implies that  $t^{(i)}$  is free and (33a) holds trivially. Finally, since we consider a partition, i.e., only one  $\gamma^{(i)}$  can be 1, (33b) must hold.  $\square$ 

## Appendix G. Proof of Proposition 1

Using the concatenated notations in Section 3.2, this reformulation follows directly from Lemma 1 with  $\mathcal{A} \triangleq H_x^i$ ,  $\mathcal{B} \triangleq \bar{p}_x^i - \bar{P}_x^i \bar{f}_x^i$ ,  $\mathcal{C} \triangleq -\bar{P}_x^i \Gamma_{xu}^i$ ,  $\mathcal{D} \triangleq H_y^i$ ,  $e \triangleq \bar{p}_y^i - \bar{P}_y^i \bar{f}_y^i$ ,  $\mathcal{F} \triangleq -\bar{P}_y^i \Gamma_{yu}^i$  and  $\mathcal{G} \triangleq H_{\bar{x}}^i$ ,  $\mathcal{L} \triangleq h_{\bar{x}}^i$ .

## Appendix H. Proof of Proposition 2

By leveraging Lemma 2, the conditional "OR" state constraints in (27a) can be reformulated as

$$\begin{split} \forall i \in \mathbb{Z}_{N}^{+}, \forall j \in \mathbb{Z}_{n_{s,i}}^{+}, \forall k \in \mathbb{Z}_{T-1}^{0}: \\ \left\{ \begin{array}{l} r_{i,k}^{(j)} \in \{0, 1\}, \text{SOS-1}: \{r_{i,k}^{(j)}, s_{i,k}^{(j)}\}, \sum_{j} r_{i,k}^{(j)} \geq 1, \\ P_{s,i}^{(j)} M_{\overline{z}_{i,k}} \overline{x}_{s,i,k}^{(j)} + P_{s,i}^{(j)} \Gamma_{xu,i,k} u_{T} - p_{s,i}^{(j)} + P_{s,i}^{(j)} \widetilde{f}_{x,i,k} \leq s_{i,k}^{(j)}, \\ \forall \overline{x}_{s,i,k}^{(j)} \in \{\overline{x}_{s,i,k}^{(j)}: P_{y,i}^{(j)} M_{\overline{y}_{i,k}} \overline{x}_{s,i,k}^{(j)} + P_{y,i}^{(j)} \Gamma_{yu,i,k} u_{T} - p_{y,i}^{(j)} + P_{y,i}^{(j)} \widetilde{f}_{y,i,k} \leq 0, H_{\overline{x},i,k} \overline{x}_{s,i,k}^{(j)} - h_{\overline{x},i,k} \leq 0 \}. \end{array} \right. \end{split}$$

Then, we obtain (35) by applying Equivalence (ii) in Lemma 1 with the following corresponding matrices:  $\mathcal{A} \triangleq P_{s,i}^{(j)} M_{\bar{\chi}_{i,k}}$ ,  $b \triangleq p_{s,i}^{(j)} - P_{s,i}^{(j)} f_{x,i,k}$ ,  $\mathcal{C} \triangleq P_{s,i}^{(j)} \Gamma_{xu,i,k}$ ,  $\mathcal{D} \triangleq P_{s,i}^{(j)} M_{\bar{v}_{i,k}}$ ,  $e \triangleq p_{v,i}^{(j)} - P_{v,i}^{(j)} f_{y,i,k}$ ,  $\mathcal{F} \triangleq -P_{v,i}^{(j)} \Gamma_{yu,i,k}$ ,  $\mathcal{G} \triangleq H_{\bar{\chi}_{i,k}}$ ,  $h \triangleq h_{\bar{\chi}_{i,k}}$ .  $\square$ 

## Appendix I. Proof of Proposition 3

By leveraging Lemma 3, the coupled state-input constraints in (27a) can be reformulated as

$$\begin{cases} & \gamma_{i,k}^{(j)} \in \{0,1\}, \, \text{SOS-1}: \{\gamma_{i,k}^{(j)}, \, t_{i,k}^{(j)}\}, \, \sum_{j} \gamma_{i,k}^{(j)} = 1, \\ & \begin{bmatrix} Q_{ux,i}^{(j)} M_{\overline{X}_{i,k}} & \left[Q_{ux,i}^{(j)} \varGamma_{xu,i,k} & Q_{uu,i}^{(j)} & 0\right] \\ P_{ux,i}^{(j)} M_{\overline{x}_{i,k}} & \left[P_{ux,i}^{(j)} \varGamma_{xu,i,k} & Q\right] & \end{bmatrix} \begin{bmatrix} \overline{x}_{i,k}^{(j)} \\ \overline{x}_{i,k} \end{bmatrix} \leq \begin{bmatrix} q_{u,i}^{(j)} - Q_{ux,i}^{(j)} \widetilde{f}_{x,i,k} \\ p_{ux,i}^{(j)} - P_{ux,i}^{(j)} \widetilde{f}_{x,i,k} \end{bmatrix} + t_{i,k}^{(j)}, \\ \forall \overline{x}_{i,k}^{(j)} \in \left\{ \overline{x}_{i,k}^{(j)} : P_{y,i}^{(j)} M_{\overline{y}_{i,k}} \overline{x}_{i,k}^{(j)} + P_{y,i}^{(j)} \varGamma_{yu,i,k} u_T - p_{y,i}^{(j)} + P_{y,i}^{(j)} \widetilde{f}_{y,i,k} \leq 0, H_{\overline{x},i,k} \overline{x}_{i,j}^{(j)} - h_{\overline{x},i,k} \leq 0 \right\}, \end{cases}$$

where the following corresponding matrices in Lemma 3 are used:  $\chi_{i,k} \triangleq \bar{\chi}_{i,k}$ ,  $y \triangleq u_T$ ,  $Q_{i,k}^{(j)} \triangleq Q_{ux,i}^{(j)} M_{\bar{\chi}_{i,k}}$ ,  $\mathcal{R}_{i,k}^{(j)} \triangleq \left[Q_{ux,i}^{(j)} \Gamma_{xu,i,k} \quad Q_{uu,i}^{(j)} \quad Q_{ux,i}^{(j)} \int_{x_i,k}^{\infty} e^{-\frac{i}{2}} P_{ux,i}^{(j)} M_{\bar{\chi}_{i,k}}^{-1}$ ,  $\mathcal{T}_{i,k}^{(j)} \triangleq \left[P_{ux,i}^{(j)} \Gamma_{xu,i,k} \quad 0\right]$ ,  $\alpha_{i,k}^{(j)} \triangleq q_{u,i}^{(j)} - Q_{ux,i}^{(j)} \tilde{\chi}_{x,i,k}$ , and  $\beta_{i,k}^{(i)} \triangleq p_{ux,i}^{(j)} - P_{ux,i}^{(j)} \tilde{\chi}_{x,i,k}^{-1}$ . We further utilize Equivalence (ii) in Lemma 1 to reformulate the coupled input–state piecewise constraints above to obtain (36), where the following matrices in Lemma 1 are used to get the result in Proposition 3:  $\mathcal{A} \triangleq \left[Q_{i,k}^{(j)T} \quad \mathcal{S}_{i,k}^{(j)T}\right]^T$ ,  $\mathcal{B} \triangleq \left[\alpha_{i,k}^{(j)T} \quad \beta_{i,k}^{(i)T}\right]^T + t_{i,k}^{(j)}\mathbb{1}$ ,  $\mathcal{C} \triangleq \left[-\mathcal{R}_{i,k}^{(j)T} - \mathcal{T}_{i,k}^{(j)T}\right]^T$ ,  $\mathcal{G} \triangleq H_{\bar{\chi},i,k}$ ,  $\mathcal{B} \triangleq h_{\bar{\chi},i,k}$ ,  $\mathcal{D} \triangleq P_{y,i}^{(j)}M_{\bar{y}_{i,k}}$ ,  $e \triangleq p_{y,i}^{(j)} - P_{y,j}^{(j)}\tilde{f}_{y,i,k}$  and  $\mathcal{F} \triangleq -P_{y,i}^{(j)}\Gamma_{yu,i,k}$ .

#### Appendix J. Proof of Proposition 4

This is obtained using the same steps in Theorem 1 of [13]. Similar to the previous result, the (non-convex) input, responsibility and safety constraints are enforced in the outer problem by Propositions 1–3; thus, they trivially hold in the inner problem of the separability condition and need not be explicitly included.  $\Box$ 

## References

- [1] V. Venkatasubramanian, R. Rengaswamy, K. Yin, S. Kavuri, A review of process fault detection and diagnosis: Part I: Quantitative model-based methods, Comp. & Chem. Eng. 27 (3) (2003) 293–311.
- [2] H. Lou, P. Si, The distinguishability of linear control systems, Nonlinear Anal. Hybrid Syst. 3 (1) (2009) 21–39.
- [3] K.M.D. Motchon, K.M. Pekpe, J.P. Cassar, S. De Bievre, Strict residual distinguishability of continuous-time switched linear systems with disturbances, IFAC-PapersOnLine 48 (21) (2015) 1268–1274.
- [4] F. Harirchi, S.Z. Yong, N. Ozay, Guaranteed fault detection and isolation for switched affine models, in: IEEE CDC, 2017, pp. 5161-5167.
- [5] Z.Y. Jin, Q. Shen, S.Z. Yong, Optimization-based approaches for affine abstraction and model discrimination of uncertain nonlinear systems, in: CDC, 2019, pp. 7976–7981.
- [6] S. Borchers, P. Rumschinski, S. Bosio, R. Weismantel, R. Findeisen, Model discrimination and parameter estimation via infeasibility certificates for dynamical biochemical reaction networks, IFAC Proc. Vol. 42 (10) (2009) 245–250.
- [7] P. Rumschinski, S. Streif, R. Findeisen, Combining qualitative information and semi-quantitative data for guaranteed invalidation of biochemical network models, Internat. J. Robust Nonlinear Control 22 (10) (2012) 1157–1173.
- [8] L.H. Chiang, E.L. Russell, R.D. Braatz, Fault Detection and Diagnosis in Industrial Systems, Springer-Verlag London, 2001.
- [9] D.M. Raimondo, R.D. Braatz, J.K. Scott, Active fault diagnosis using moving horizon input design, in: ECC, 2013, pp. 3131-3136.
- [10] R. Nikoukhah, S. Campbell, Auxiliary signal design for active failure detection in uncertain linear systems with a priori information, Automatica 42 (2) (2006) 219–228.
- [11] J.K. Scott, R. Findeison, R.D. Braatz, D.M. Raimondo, Input design for guaranteed fault diagnosis using zonotopes, Automatica 50 (6) (2014) 1580–1589.
- [12] S. Cheong, I.R. Manchester, Input design for discrimination between classes of LTI models, Automatica 53 (2015) 103-110.

- [13] Y. Ding, F. Harirchi, S.Z. Yong, E. Jacobsen, N. Ozay, Optimal input design for affine model discrimination with applications in intention-aware vehicles, in: ACM/IEEE ICCPS, 2018, pp. 5161–5167.
- [14] K. Singh, Y. Ding, N. Ozay, S.Z. Yong, Input design for nonlinear model discrimination via affine abstraction, IFAC-PapersOnLine 51 (16) (2018) 175–180
- [15] R. Niu, Q. Shen, S.Z. Yong, Partition-based parametric active model discrimination with applications to driver intention estimation, in: ECC, 2019, pp. 3880–3885.
- [16] O. Shen, S.Z. Yong, Active model discrimination using partition-based output feedback, in: ECC, 2020, pp. 712-717.
- [17] F. Harirchi, S.Z. Yong, E. Jacobsen, N. Ozay, Active model discrimination with applications to fraud detection in smart buildings, IFAC-PapersOnline 50 (1) (2017) 9527–9534.
- [18] O. Stein, How to solve a semi-infinite optimization problem, European J. Oper. Res. 223 (2) (2012) 312-320.
- [19] Inc. Gurobi Optimization, Gurobi optimizer reference manual, 2015, URL http://www.gurobi.com.
- [20] IBM ILOG CPLEX, V12, 1: User's manual for CPLEX, Int. Bus. Mach. Corp. 46 (53) (2009) 157,
- [21] J. Löfberg, YALMIP: A toolbox for modeling and optimization in MATLAB, in: CACSD, Taipei, Taiwan, 2004, URL http://users.isy.liu.se/johanl/valmip.
- [22] M. Kvasnica, P. Grieder, M. Baotić, Multi-parametric toolbox (MPT), 2004, URL http://control.ee.ethz.ch/~mpt/.
- [23] X.Q. Liu, H.Y. Zhang, J. Liu, J. Yang, Fault detection and diagnosis of permanent-magnet DC motor based on parameter estimation and neural network, IEEE Trans. Ind. Electron. 47 (5) (2000) 1021–1030.
- [24] T. Kara, I. Eker, Nonlinear closed-loop direct identification of a DC motor with load for low speed two-directional operation, Electr. Eng. 86 (2) (2004) 87-96.
- [25] D. Bertsimas, D.B. Brown, C. Caramanis, Theory and applications of robust optimization, SIAM Rev. 53 (3) (2011) 464-501.
- [26] A. Ben-Tal, L. El Ghaoui, A. Nemirovski, Robust Optimization, Princeton University Press, 2009.